Magnetic small–angle neutron scattering of nanostructured ferromagnets

Dirk Honecker, Institut Laue-Langevin

PNPI School on Condensed State Physics,15/03/2016

Outline

Small–Angle Neutron Scattering (SANS)

a technique to study the microstructure at nanometer scales

Micromagnetics

Theory for magnetic SANS of multiphase bulk ferromagnets

Experimental Results on nanostructured ferromagnets

Nanocrystalline magnetic alloys

Co nanowire array

Summary and conclusion

Small–Angle Neutron Scattering (SANS) diffractometer

3 SANS instruments (D11, D22, D33) at ILL

SANS probes bulk material on nanometer length scale (1-500 nm)

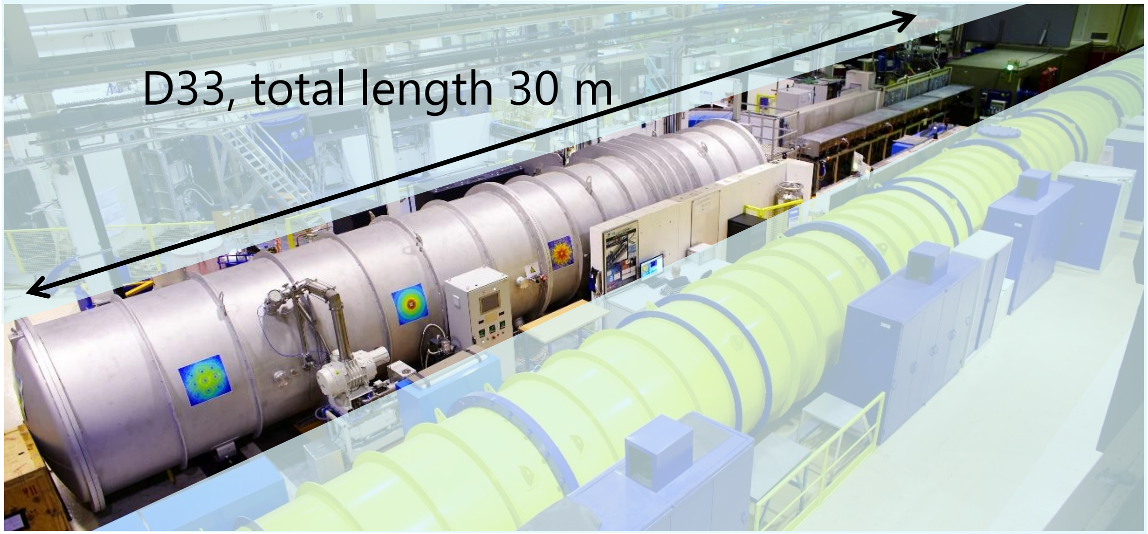

Science cases on D33

Soft condensed matter
Colloids, polymers, gels,
liquid crystals,
self assembly of molecules

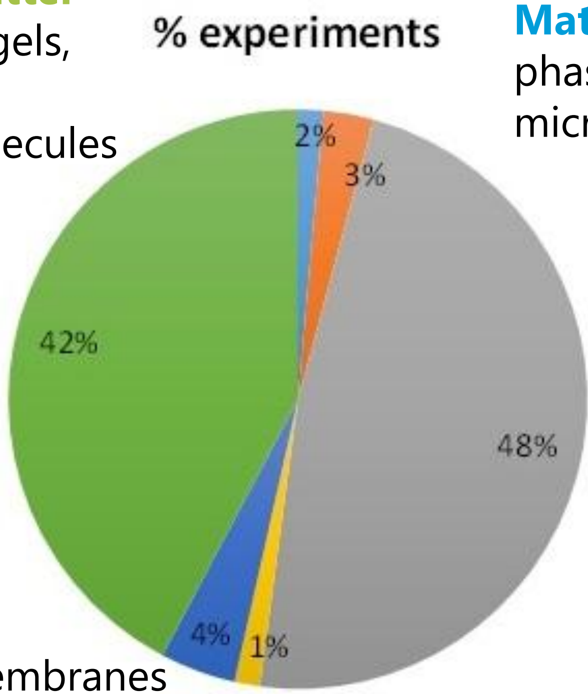

Material Science
phase separation in alloys and glasses,
microporosity

Magnetism and Microstructure
Flux line lattices in superconductors
Chiral magnetic phases (cf. evening session)
Magnetic nanoparticles, e.g. ferrofluids
Magnetic correlations in bulk ferromagnets

Biology
proteins, membranes
vectors for drug delivery

Sample environments
- Pressure cells
- Oven
- Rheometer
- Cryostats + Dilution refrigerators
- Magnets (up to 17T)
- ...

D33: Schematic drawing

(25 K moderated)
neutron spectrum
2<λ [nm]<40

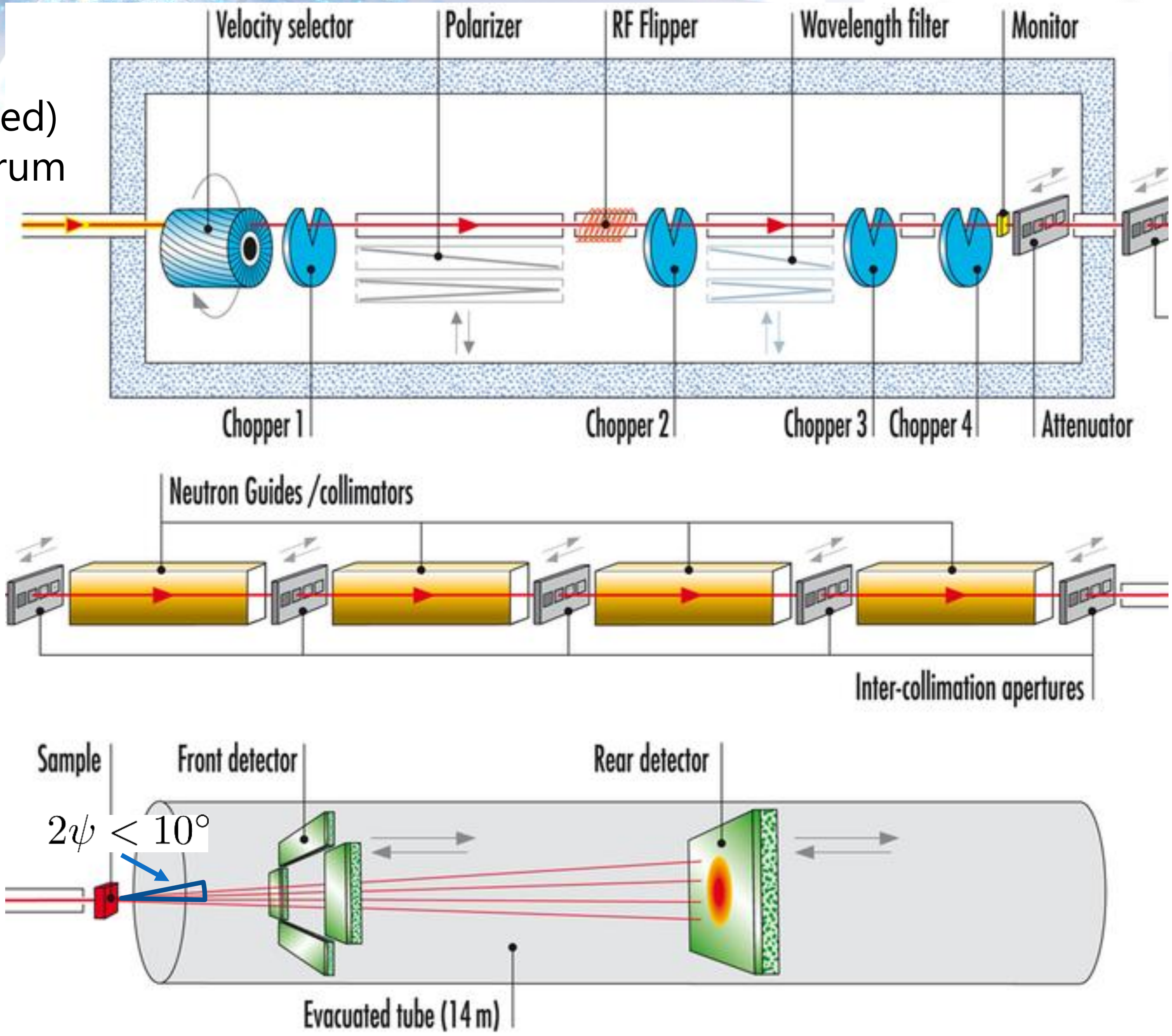

Scattered intensity

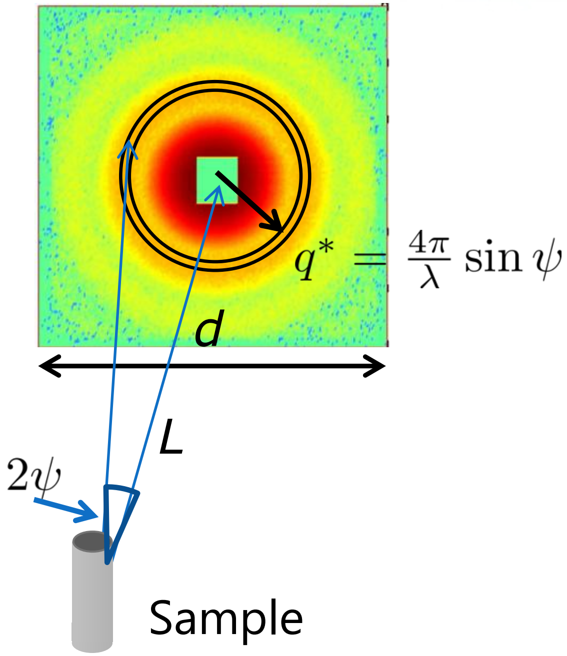

Scattering of dilute, noninteracting spheres

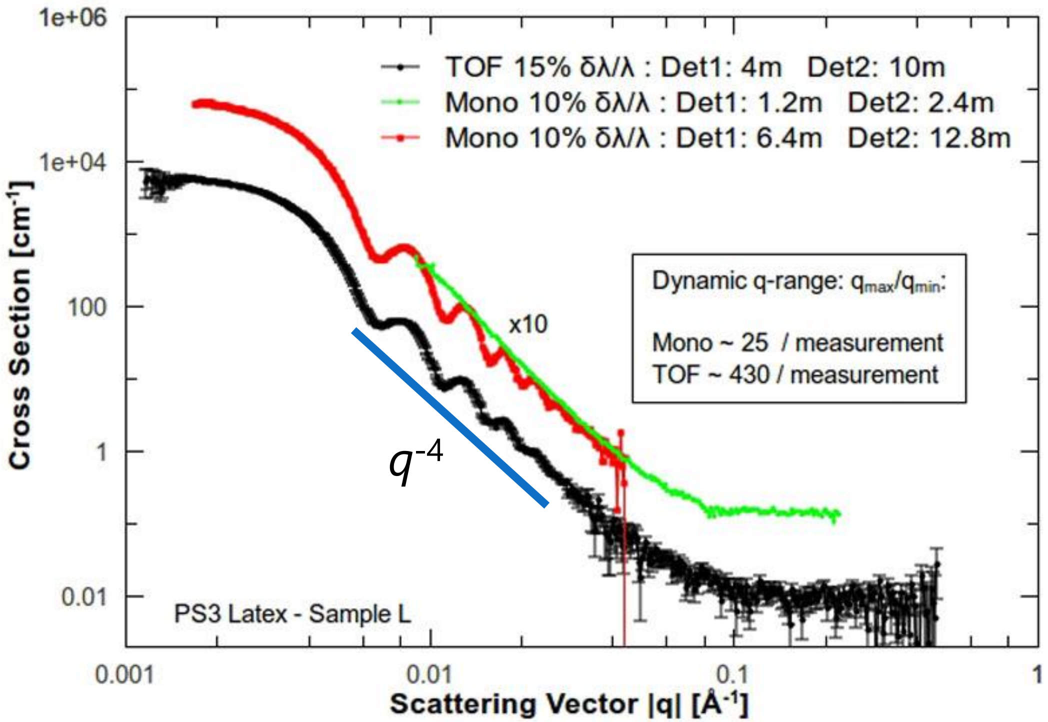

-Covered *q*-range given by sample-detector distance *L*, detector size *d* & wavelength *λ*
-Smearing of features due to polydispersity and *q* resolution

$$\Delta q^2 \approx q^2 \left(\frac{\Delta\lambda}{\lambda}\right)^2 + \left(\frac{4\pi}{\lambda}\right)^2 \Delta\psi^2$$

Small–Angle Neutron Scattering (SANS)

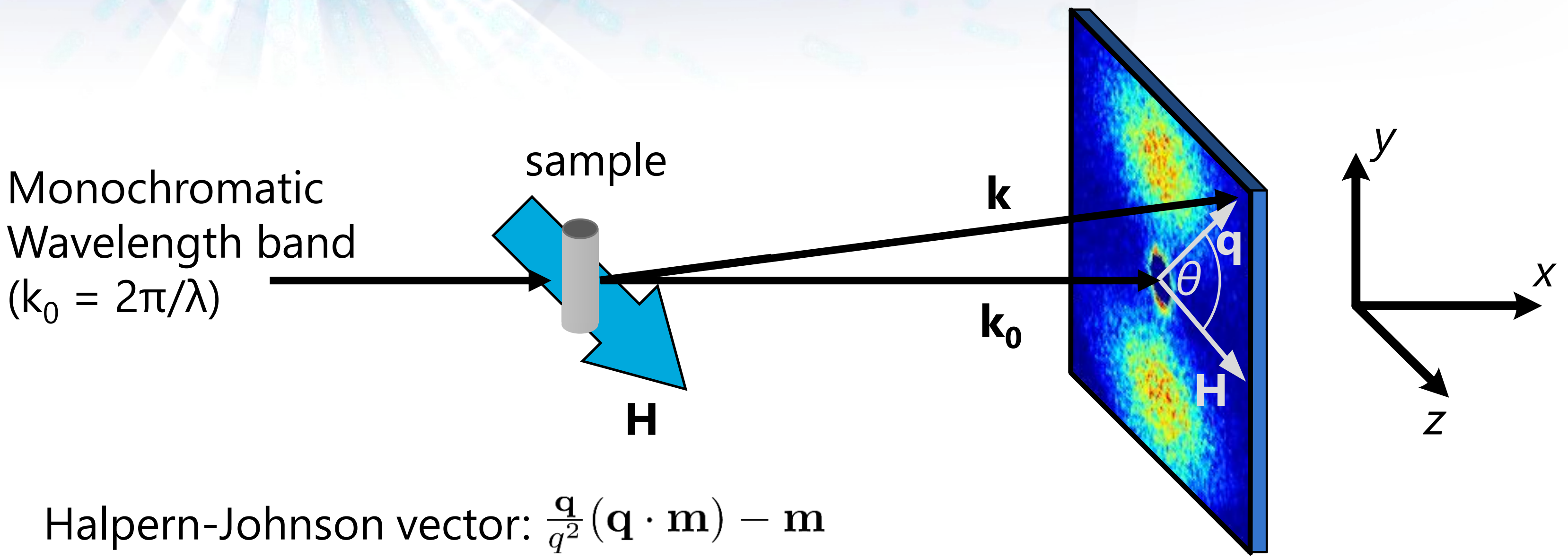

Halpern-Johnson vector: $\frac{\mathbf{q}}{q^2}(\mathbf{q}\cdot\mathbf{m})-\mathbf{m}$
Only magnetization component perpendicular to q is effective in magnetic neutron scattering

unpolarised small–angle scattering cross section $(\mathbf{k}_0 \perp \mathbf{H}) \rightarrow \mathbf{q} = (0, q_y, q_z)$

$$\frac{d\Sigma}{d\Omega}(\mathbf{q}) \propto |\widetilde{N}|^2 + |\widetilde{M}_z|^2 \sin^2\theta + |\widetilde{M}_x|^2 + |\widetilde{M}_y|^2 \cos^2\theta - 2\widetilde{M}_y\widetilde{M}_z \sin\theta\cos\theta$$

mixture of nuclear and magnetic scattering

Magnetic small-angle neutron scattering

Dilute magnetic particles in nonmagnetic matrix
(e.g. ferrofluids, magnetic precipitate)

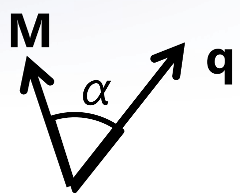

$$\frac{d\Sigma_{\mathrm{mag}}}{d\Omega}(q,H) = \frac{N}{V} V_p^2 |F(\mathbf{q})|^2 [(\Delta\rho_M)^2 \langle \sin^2\alpha \rangle]$$

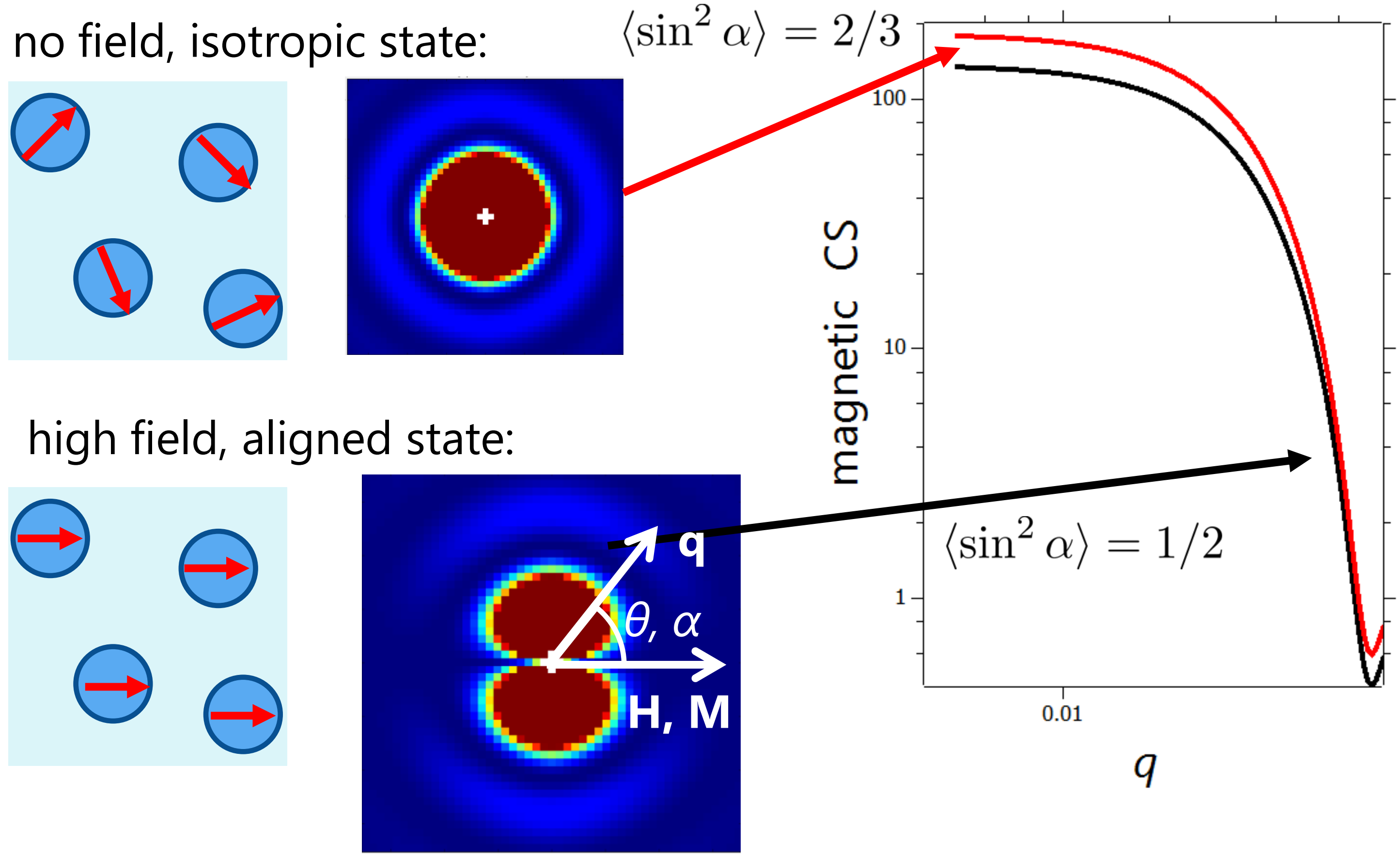

Production process of nanocrystalline magnetic alloys

rapid solidification

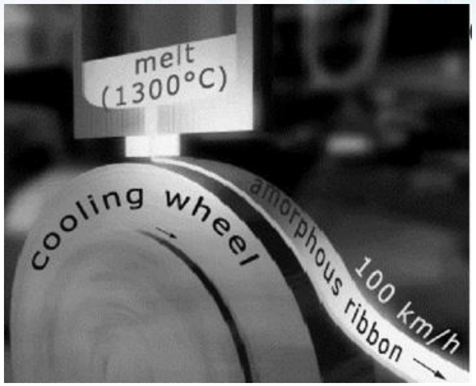

G. Herzer, Acta Materialia 61, 718 (2013)

bright-field TEM of NANOPERM alloy

C.F. Conde, Acta Mater. 55, 5675 (2007)

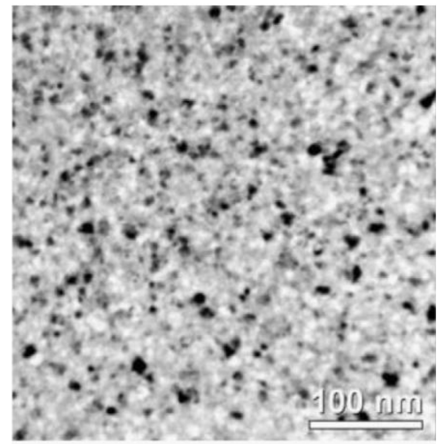

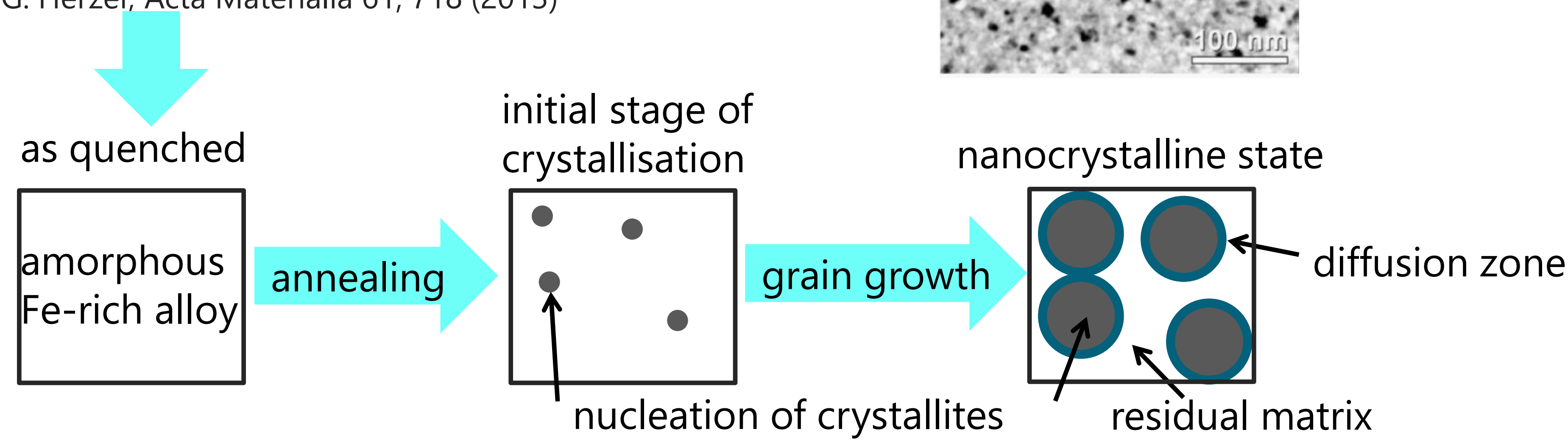

Magnetic SANS at high magnetic field

Material: $(Fe_{0.985}Co_{0.015})_{90}Zr_7B_3$; particle size D = 15±2 nm; particle volume $\eta \approx 65$ %

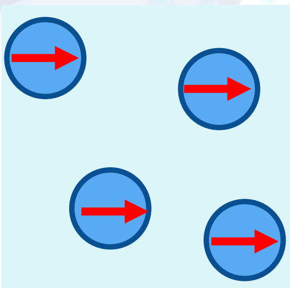

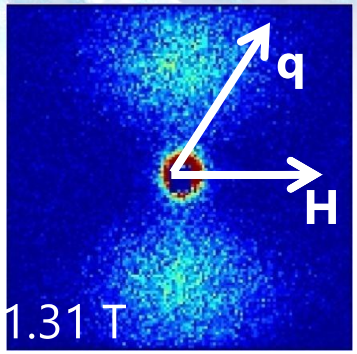

$$\frac{d\Sigma}{d\Omega}(\mathbf{q}) \propto |\widetilde{N}|^2 + |\widetilde{M}_z|^2 \sin^2\theta$$

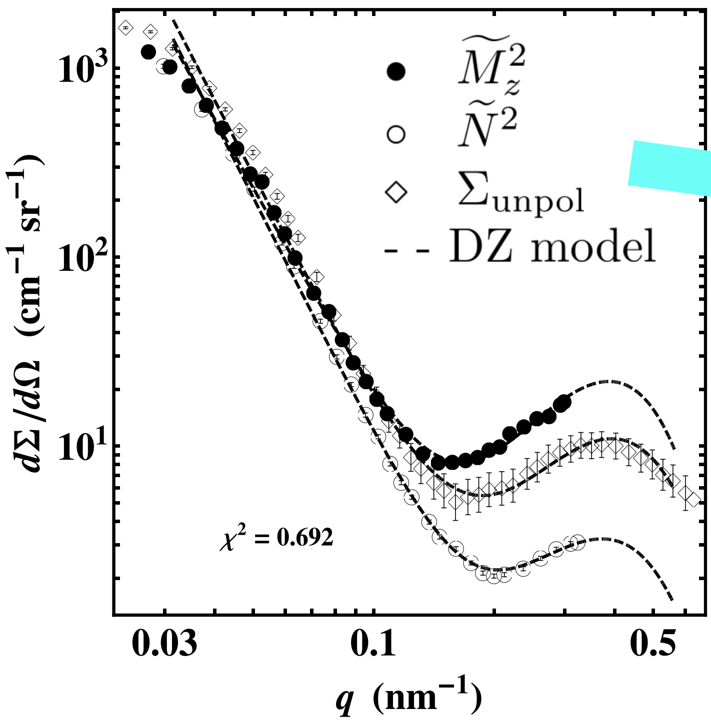

SLD profile from particle-core model

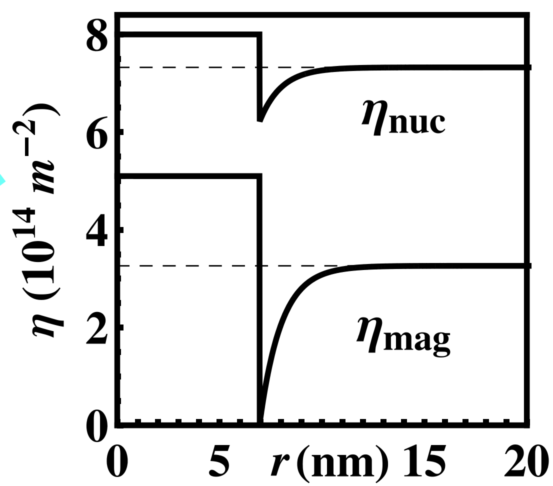

- mean particle size D_{DZ} = 14 nm
- size of diffusion zone ~ 1 nm

Magnetic microstructure of nanocrystalline ferromagnet

- 3D bulk material with crystallite size D ~10 – 20 nm
- two ferromagnetic phases (exchange coupled)
- random orientation of crystallographic axes
- high volume fraction of internal interfaces
- jump in M_s at interfaces

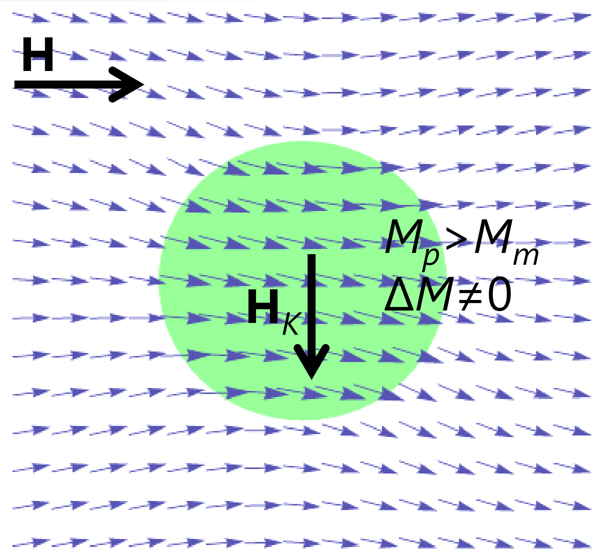

Magnetic microstructure is highly inhomogeneous
- spin disordered on nm-scale
- crossing length scales scenario
- important for coercivity, remanence, …
- (field dependent) spin-misalignment SANS

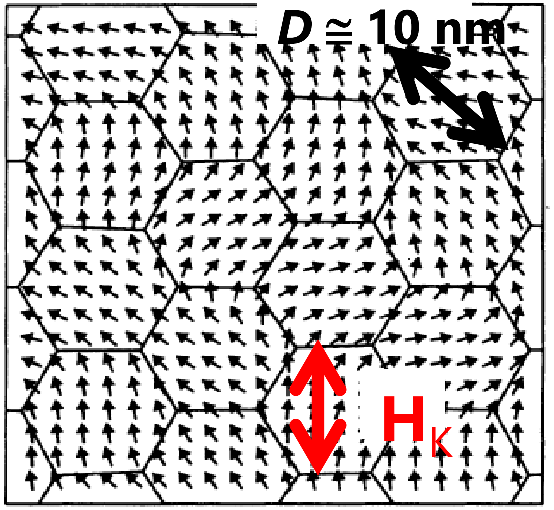

T. Schrefl *et al.*, PRB 49, 6100 (1994).

Field dependent Small–Angle Neutron Scattering (SANS)

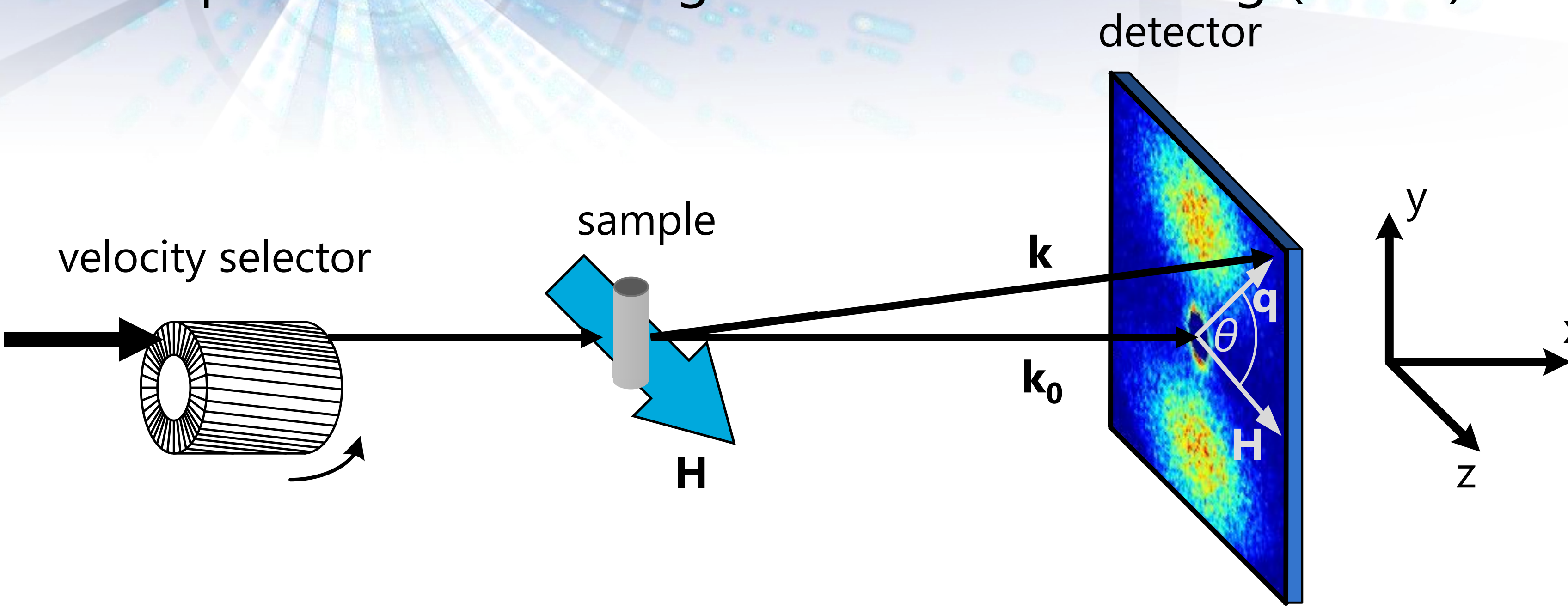

unpolarised small–angle scattering cross section $(\mathbf{k}_0 \perp \mathbf{H})$

$$\frac{d\Sigma}{d\Omega}(\mathbf{q}) \propto \cancel{|\widetilde{N}|^2 + |\widetilde{M}_z|^2 \sin^2\theta} + |\widetilde{M}_x|^2 + |\widetilde{M}_y|^2 \cos^2\theta - 2\widetilde{M}_y \widetilde{M}_z \sin\theta \cos\theta$$

difference data → spin-misalignment scattering

Spin-Misalignment Scattering of NANOPERM

Material: $Fe_{89}Zr_7B_3Cu_1$; particle size D = 12±2 nm; particle volume $\eta \approx$ 40 %

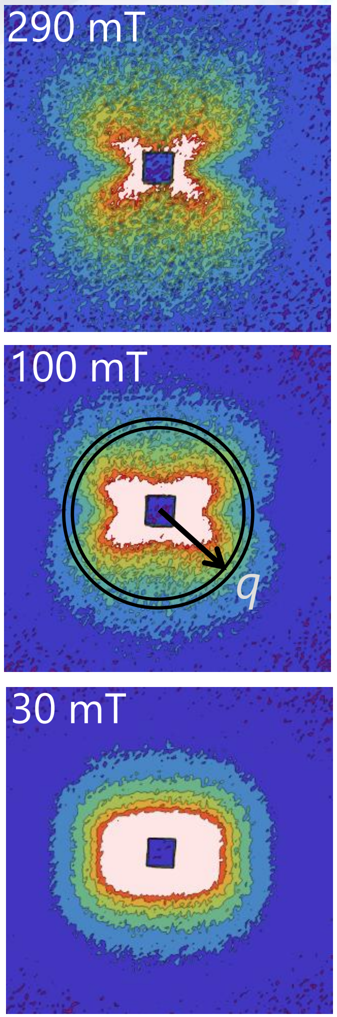

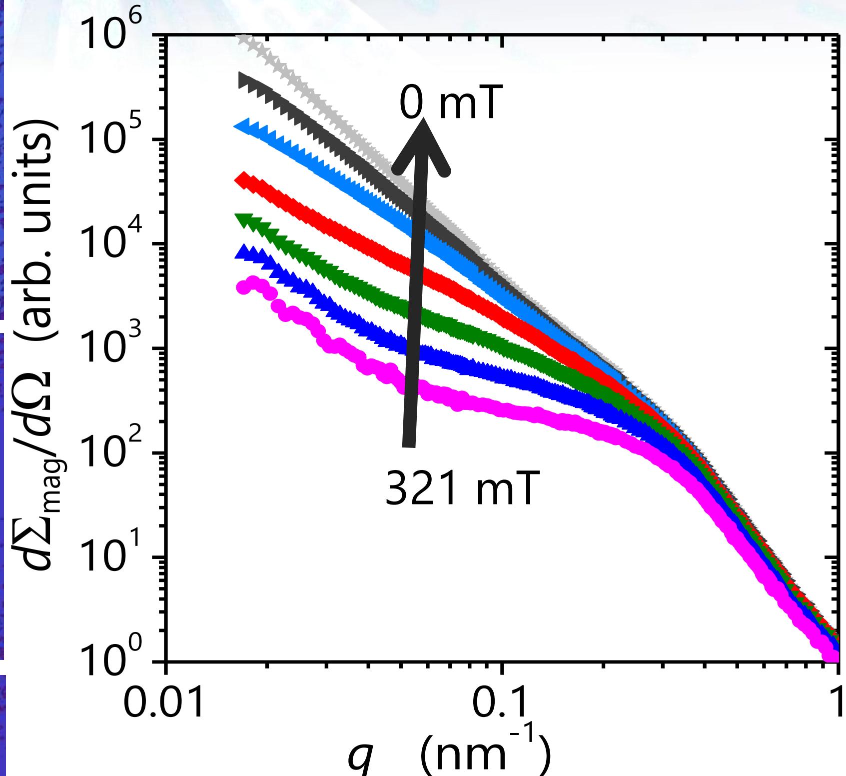

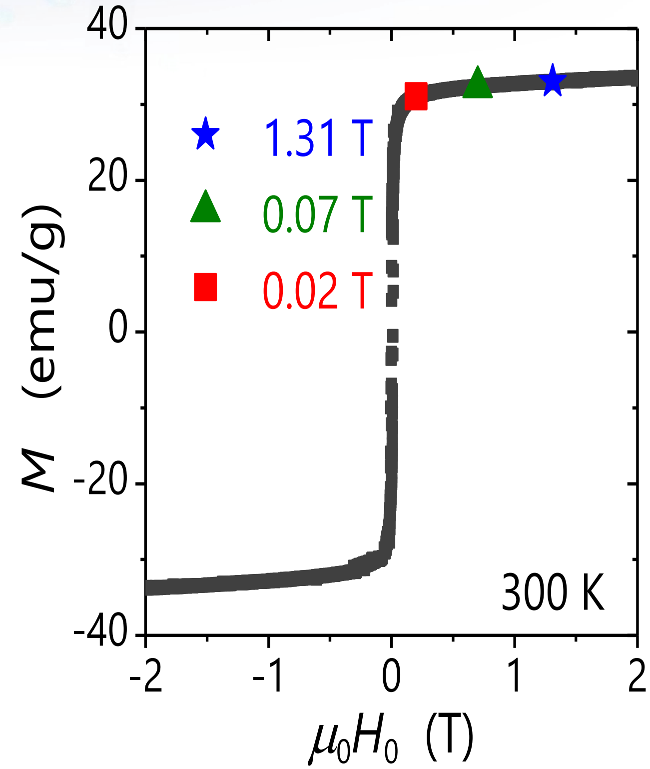

$$\frac{d\Sigma_{mag}}{d\Omega}(\mathbf{q}) \propto |\widetilde{M}_x|^2 + |\widetilde{M}_y|^2 \cos^2\theta - 2\widetilde{M}_y \widetilde{M}_z \sin\theta\cos\theta$$

strong, field-dependent magnetic scattering

Clover-leaf anisotropy

magnetic nanocomposites
(e.g. NANOPERM)

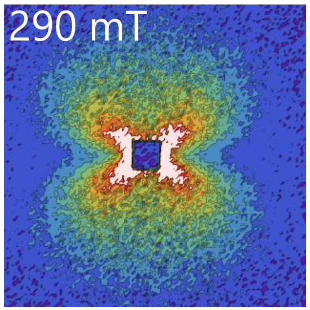

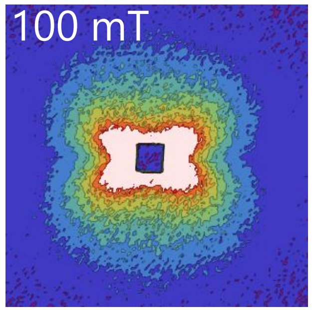

Sources of spin disorder:
Spatial variation of
- magnetic anisotropy field $\mathbf{H}_K(\mathbf{r})$
- saturation magnetisation $M_s(\mathbf{r})$

How do theses perturbations affect $\widetilde{M}_{x,y,z}(\mathbf{q}, H, A, D, \ldots)$ and $\frac{d\Sigma}{d\Omega}(\mathbf{q})$?

Micromagnetics

numerical simulation

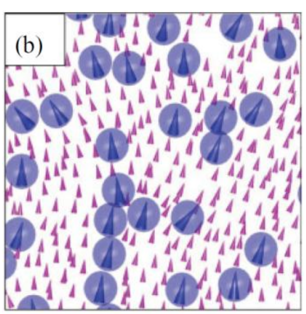

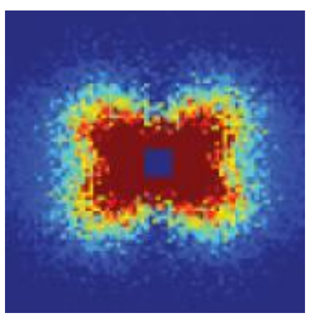

S. Erokhin, Phys. Rev. B 85, 024410 (2012)

analytical description

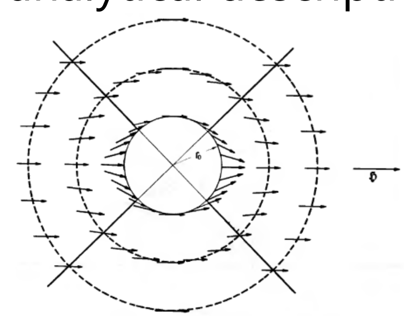

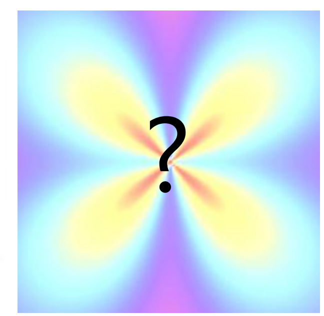

H. Kronmüller, Z. Physik 168, 478 (1962)

Micromagnetism

balance of torques (Brown, 1963)

$$[\mathbf{H} + \mathbf{H}_D(\mathbf{r}) + \mathbf{H}_K(\mathbf{r}) + \frac{2A}{\mu_0 M_s^2}\nabla^2\mathbf{M}(\mathbf{r})] \times \mathbf{M}(\mathbf{r}) = 0$$

$$M_{x,y}(\mathbf{r}) \ll M_z(\mathbf{r})$$

Compare e.g.: E. Schlömann, J. Appl. Phys. 38, 5027 (1967)
H. Kronmüller and J. Ulner, J. Magn. Magn. Mater. 6, 52 (1977)

linearised solution in the approach to saturation

magnetic anisotropy field $\propto H_K$

magnetostatic dipolar fields due to magnetisation jumps at internal interfaces $\propto \Delta M = M_p - M_m$

$$\widetilde{M}_x(\mathbf{q}, H) = \frac{(p + \frac{q_y^2}{q^2})\widetilde{H}_{K,x}(\mathbf{q}) - \frac{q_x q_y}{q^2}\widetilde{H}_{K,y}(\mathbf{q}) - p\frac{q_x q_z}{q^2}\widetilde{M}_z(\mathbf{q})}{p(p + \frac{q_x^2 + q_y^2}{q^2})}$$

$$\widetilde{M}_y(\mathbf{q}, H) = \frac{(p + \frac{q_x^2}{q^2})\widetilde{H}_{K,y}(\mathbf{q}) - \frac{q_x q_y}{q^2}\widetilde{H}_{K,x}(\mathbf{q}) - p\frac{q_y q_z}{q^2}\widetilde{M}_z(\mathbf{q})}{p(p + \frac{q_x^2 + q_y^2}{q^2})}$$

$$\widetilde{M}_z(\mathbf{q}) = (M_p - M_m)\sum_{i,j} e^{i\mathbf{q}(\mathbf{r}_i - \mathbf{r}_j)}$$

$$p(q, H) = H(1 + l_H^2 q^2)/M_s$$
$$l_H(H) = \sqrt{2A/(\mu_0 M_s H)}$$

- analytical expressions for $\widetilde{M}_x$, $\widetilde{M}_y$
- ratio H_K/ ΔM determines $\frac{d\Sigma}{d\Omega}(\mathbf{q}, H)$

D. Honecker and A. Michels,
Phys. Rev. B 87, 224426 (2013)

Comparison to experiment: NANOPERM (2D data)

Material: $Fe_{89}Zr_7B_3Cu_1$; particle size D = 12±2 nm; particle volume $\eta \approx 40$ %

experiment

theory

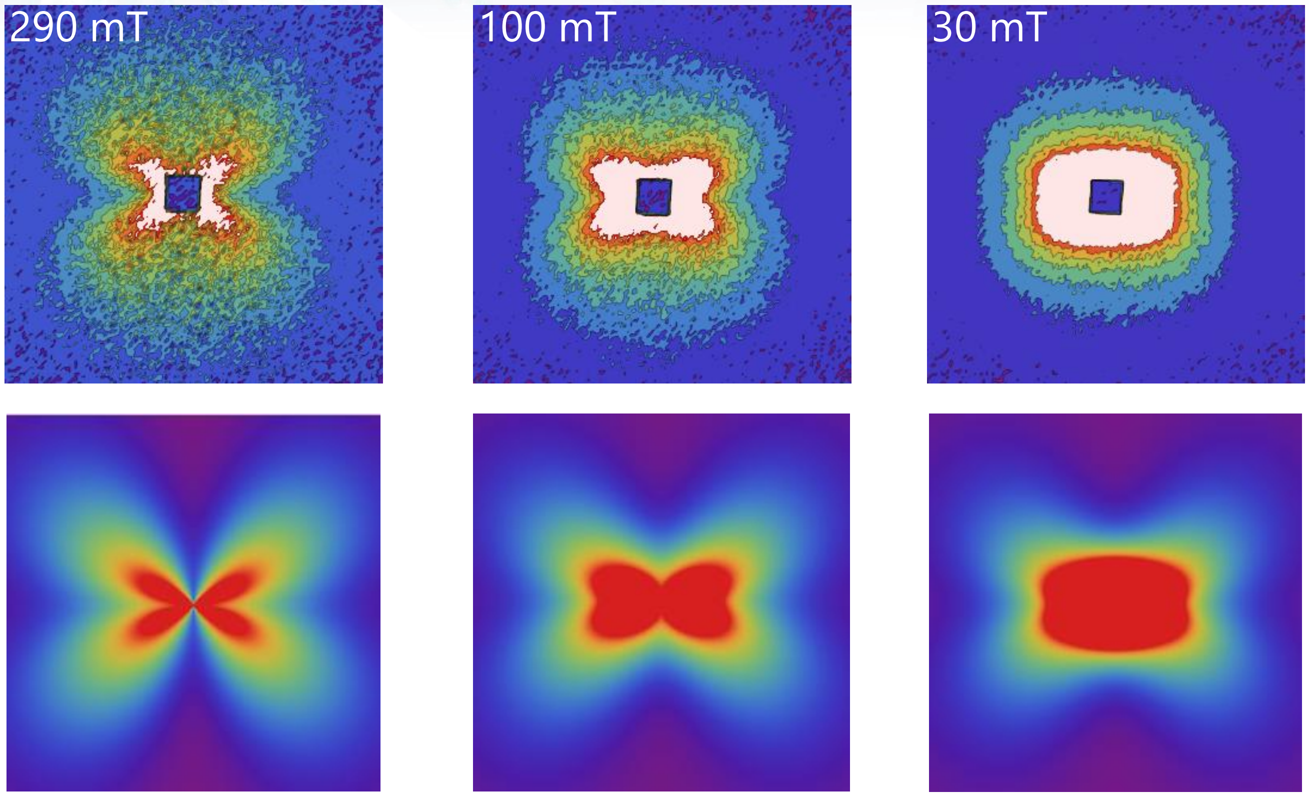

high *H*: dominated by ΔM low *H*: dominated by H_K

$$\frac{d\Sigma_{\mathrm{mag}}}{d\Omega}(q,\theta,H) \propto H_K^2\, R_K(q,\theta,H) + \Delta M^2\, R_M(q,\theta,H)$$

Field-dependent SANS of NANOPERM

$$\frac{d\Sigma_{\mathrm{mag}}}{d\Omega}(q,H) \propto H_K^2\, R_K(q,H) + \Delta M^2\, R_M(q,H)$$

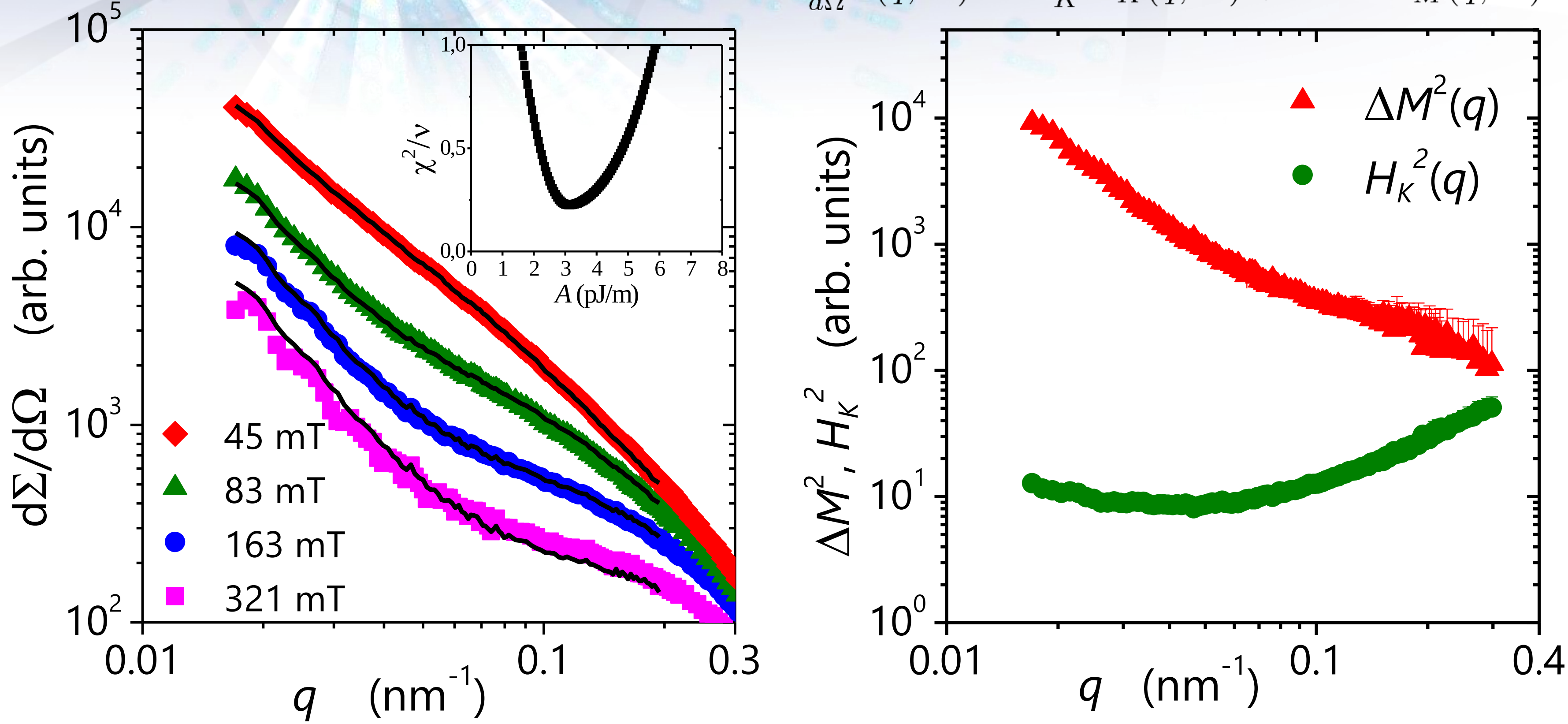

- exchange stiffness constant *A*= 3.1±0.1 pJ/m
- Δ*M* causes major part of magnetic SANS

$$\langle|\mathbf{H}_K|^2\rangle = \frac{1}{2\pi^2 b_H^2}\int_0^\infty H_K^2(q)\, q^2\, dq$$

quadratic mean anisotropy field

$$\langle|\mathbf{H}_K|^2\rangle^{1/2} \geq 10\,\mathrm{mT}$$

magnetisation magnitude fluctuations

$$\langle|M_z|^2\rangle^{1/2} \geq 50\,\mathrm{mT}$$

Correlation function of spin-misalignment scattering

$$C(r,H) \propto \frac{1}{r}\int_0^\infty \frac{d\Sigma_{\mathrm{mag}}}{d\Omega}(q,H)\,\sin(qr)\,q\,dq$$

A. Michels *et al.*, PRL 91, 267204 (2003)
A. Michels, PRB 82, 024433 (2010)

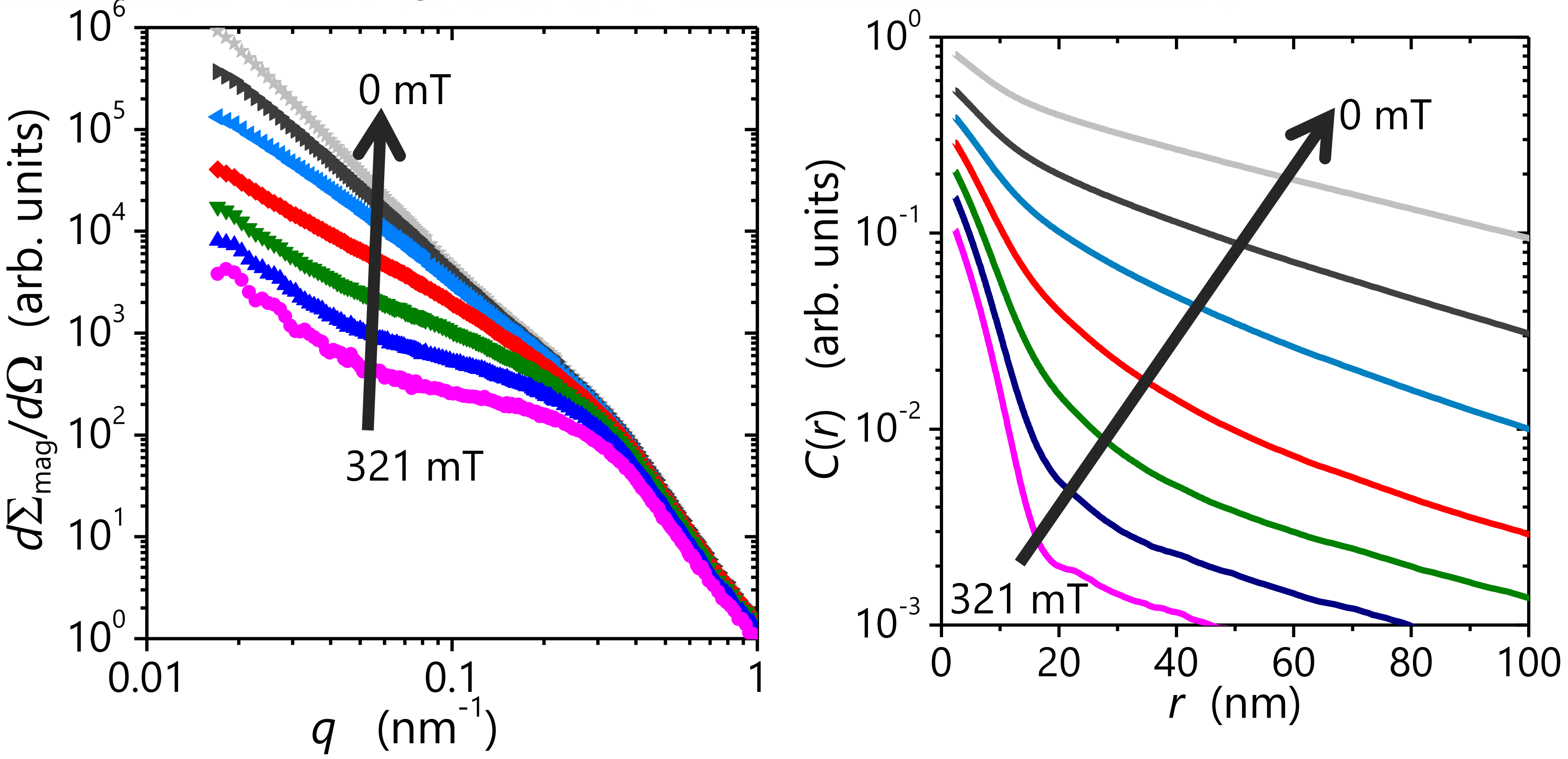

Correlation function of spin-misalignment scattering

normalised correlation function

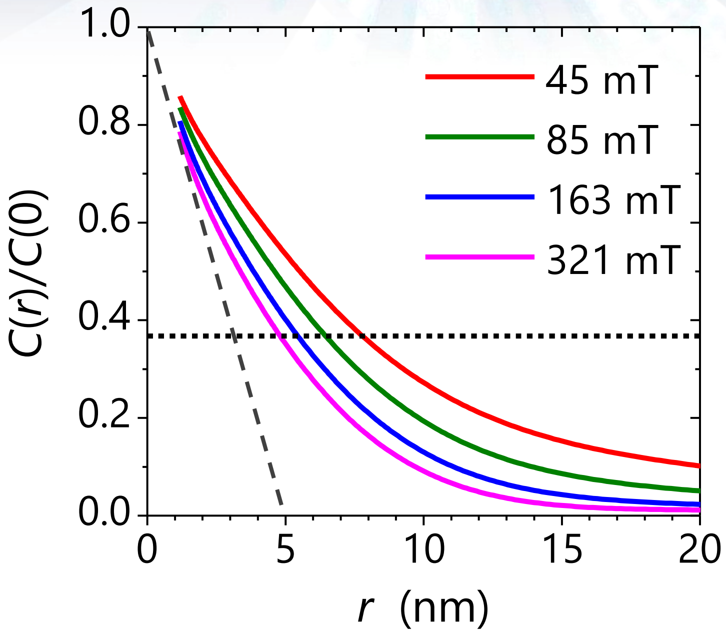

$$C(l_C) = C_0/e$$

field-dependence of decay length l_C

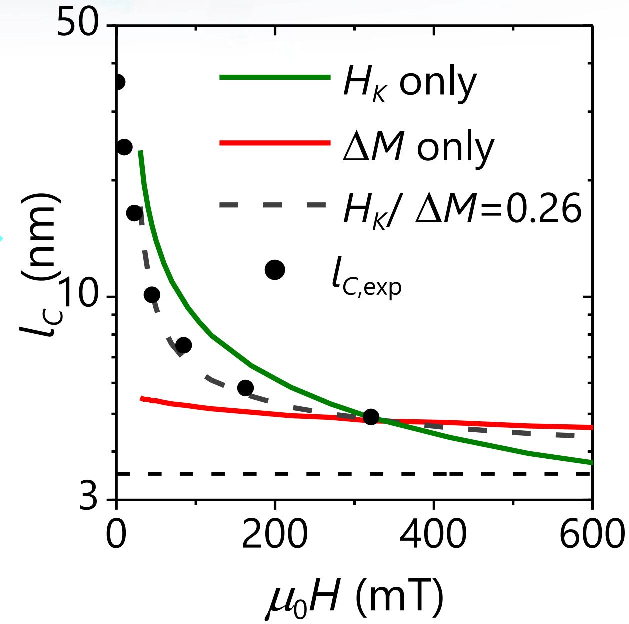

$$l_C(H) = \mathcal{L} + l(H)$$

- magnetic anisotropy scattering exhibits long-range fluctuations
- scattering due to ΔM is short-range and persistent over wide field range

- ratio H_K / ΔM determines $l_C(H)$
- $l_C(H)$ approaches 4 nm for H >1

Hard magnets: Nd-Fe-B nanocomposite

Material: nominal composition $Nd_5Fe_{74}Cr_3B_{18}$

- $Nd_2Fe_{14}B$ particle size D = 22 nm; particle volume $\eta \approx 45$ %
- Fe_3B, soft magnetic, grain size D = 29 nm J.-P. Bick et al., APL 102, 022415 (2013)

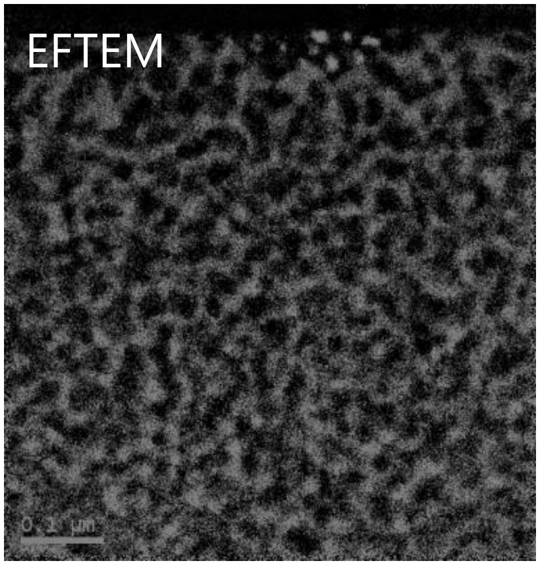

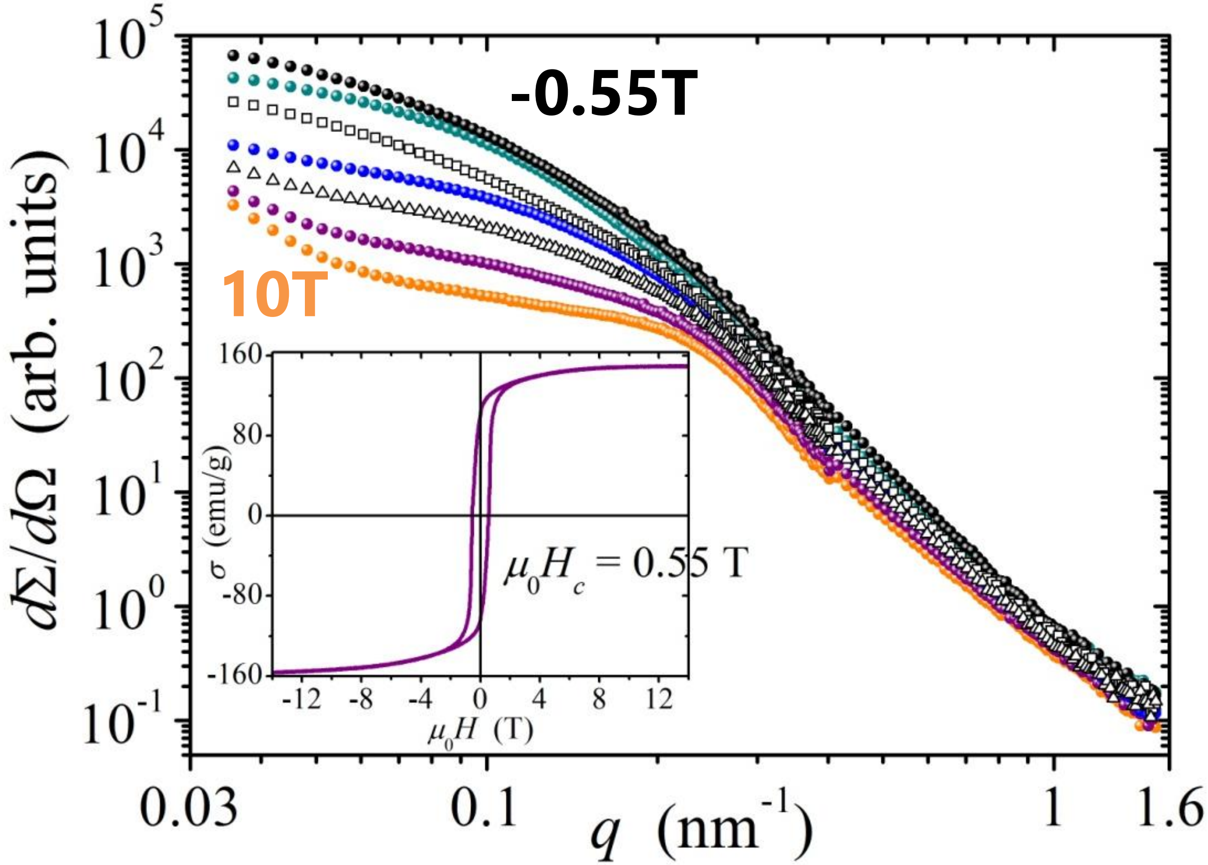

Magnetization reversal in Nd-Fe-B nanocomposites

Material: Hard magnetic nanocomposite ($Nd_5Fe_{74}Cr_3B_{18}$) J.-P. Bick et al., APL 102, 022415 (2013)

- $Nd_2Fe_{14}B$ particle size D = 22 nm; particle volume $\eta \approx 45$ %
- Fe_3B, soft magnetic, grain size D = 29 nm

spin-misalignment SANS

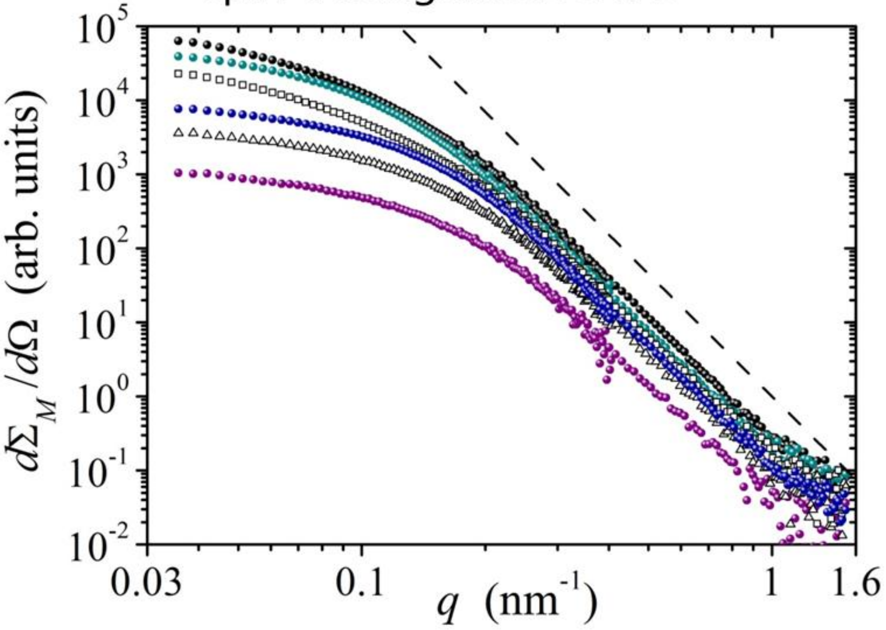

correlation function of the spin-misalignment

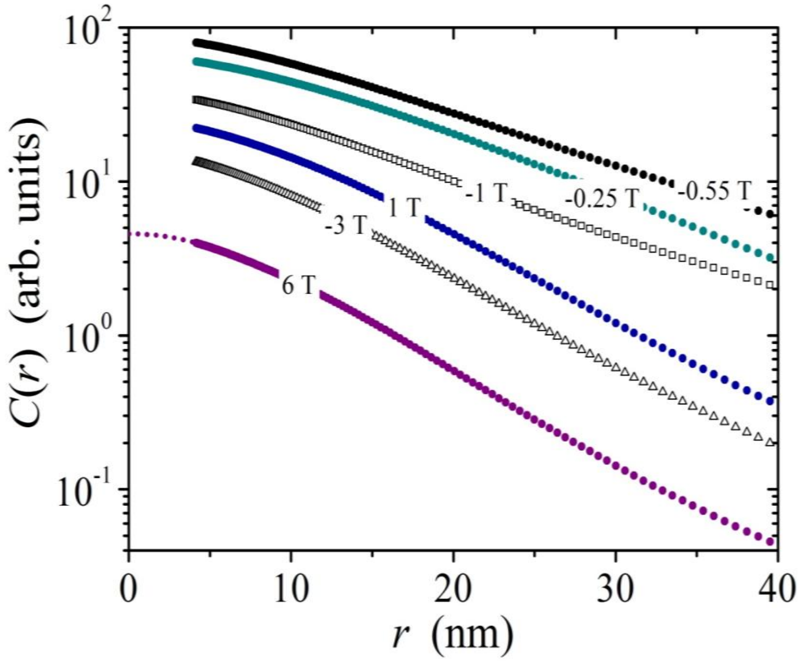

What is the spin-misalignment length during magnetization reversal?

Magnetization reversal in Nd-Fe-B nanocomposites

correlation function of the spin-misalignment

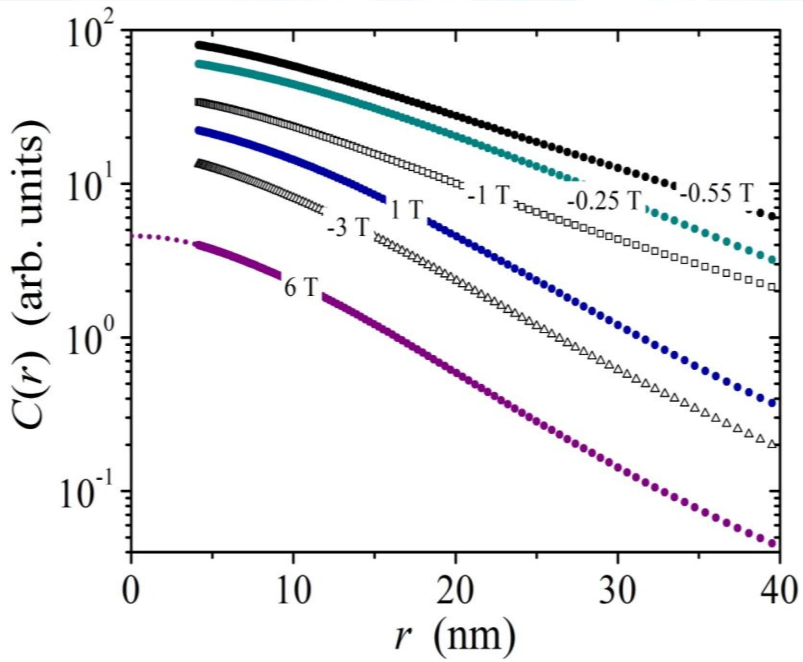

spin-misalignment length l_C

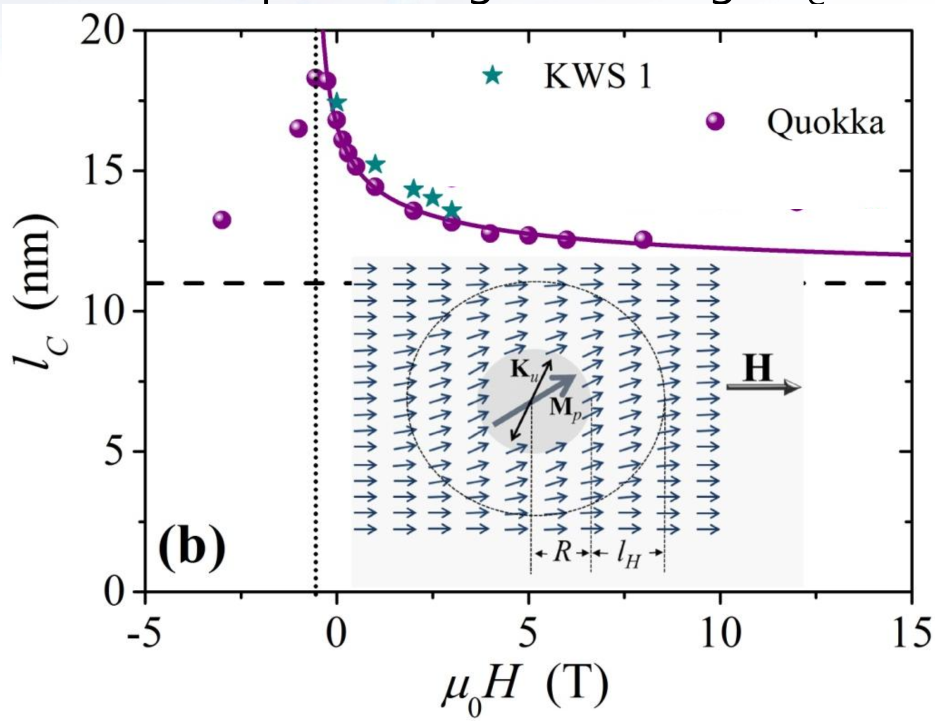

Only perturbations due to magnetic anisotropy

$$|\widetilde{M}_z(\mathbf{q})| \propto \Delta M_s = 0.01\,\mathrm{T}$$

$$l_C(H) = L + l_H(H) = L + \sqrt{\frac{2A}{\mu_0 M_s (H + H^*)}}$$

- exchange stiffness constant A= 12 pJ/m

Co nanowire array: saturated state

Pulsed electrodeposition of Co in nanoporous Al_2O_3
(d ~ 27 nm, d_{CC} ~ 48 nm, l ~ 480 nm)

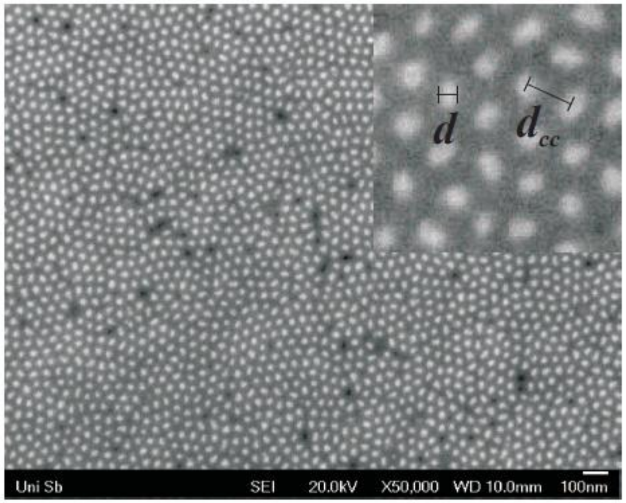

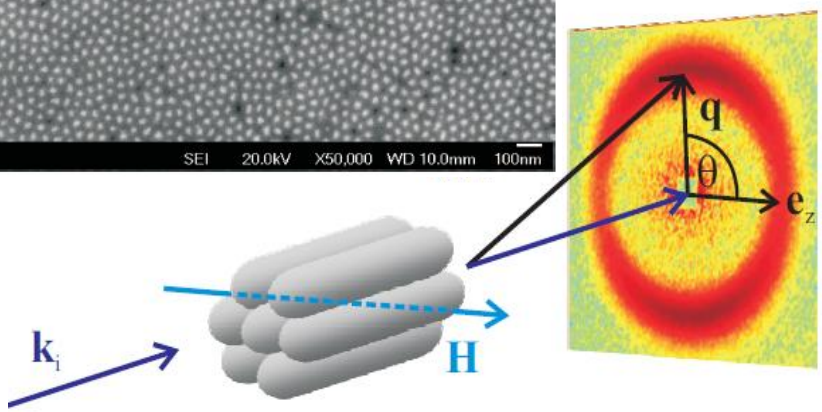

$$\frac{d\Sigma_{\rm sat}}{d\Omega} = |N(\mathbf{q})|^2 + |M_z(\mathbf{q})|^2 \sin^2\theta$$

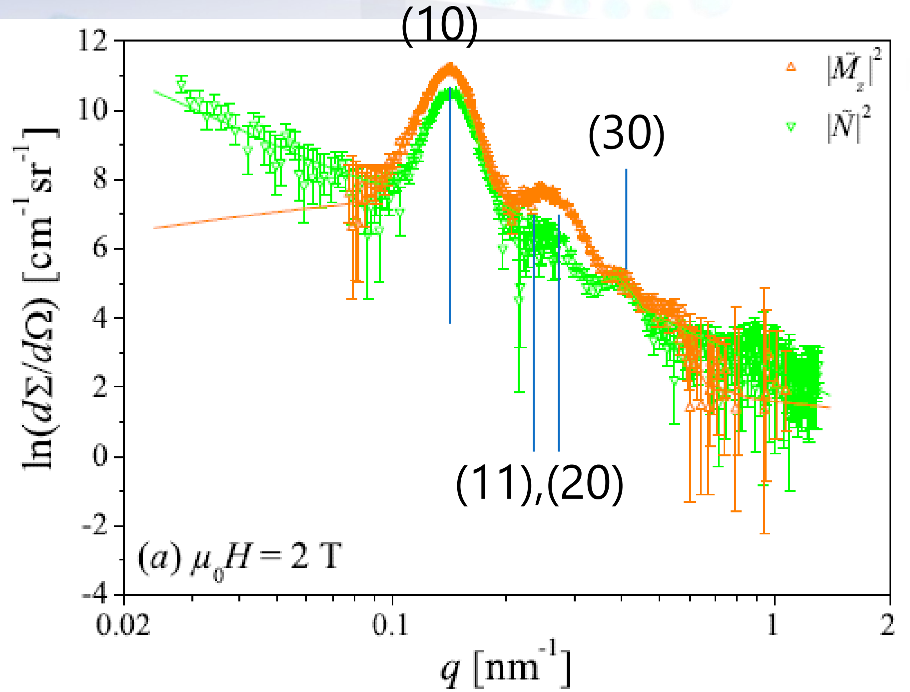

	$\lvert\tilde{N}\rvert^2$	$\lvert\tilde{M}_z\rvert^2$
R [nm]	14.6 ± 0.3	15.8 ± 0.1
d_{cc} [nm]	49.6 ± 0.1	50.0 ± 0.2

Cross section for oriented and densely packed cylinders:

$$I(q) = A|2J_1(qR)/(qR)|^2 \times (\textstyle\sum_i a_i \exp[-(q-q_i)^2/2\sigma_i^2])$$

Form factor — Structur factor of hexagonal order

Co nanowire array: field dependence

Pulsed electrodeposition of Co in nanoporous Al_2O_3
(d ~ 27 nm, d_{CC} ~ 48 nm, L ~ 480 nm)

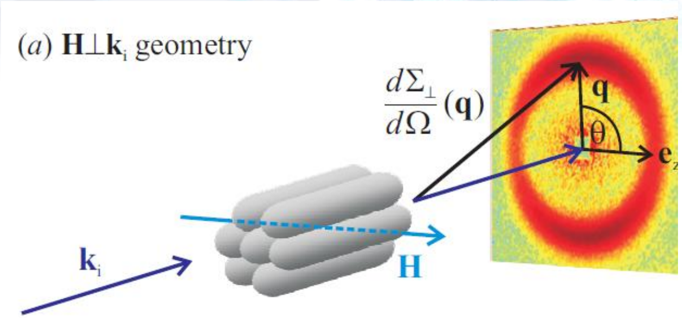

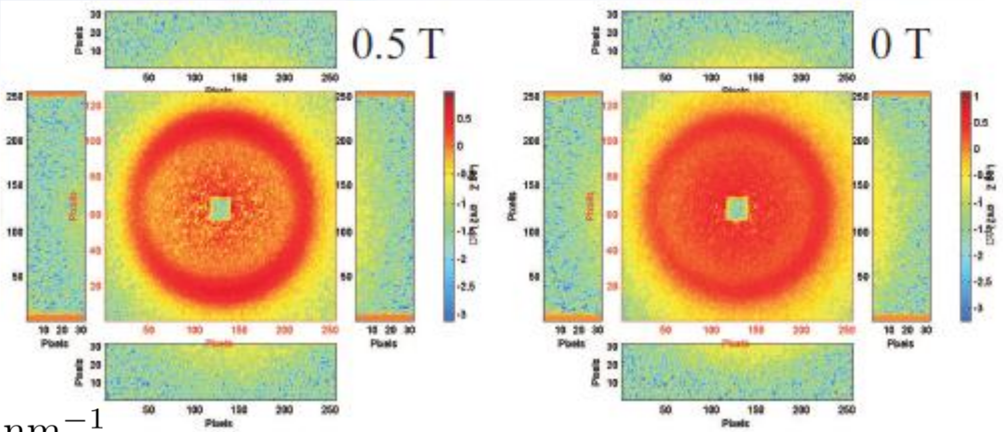

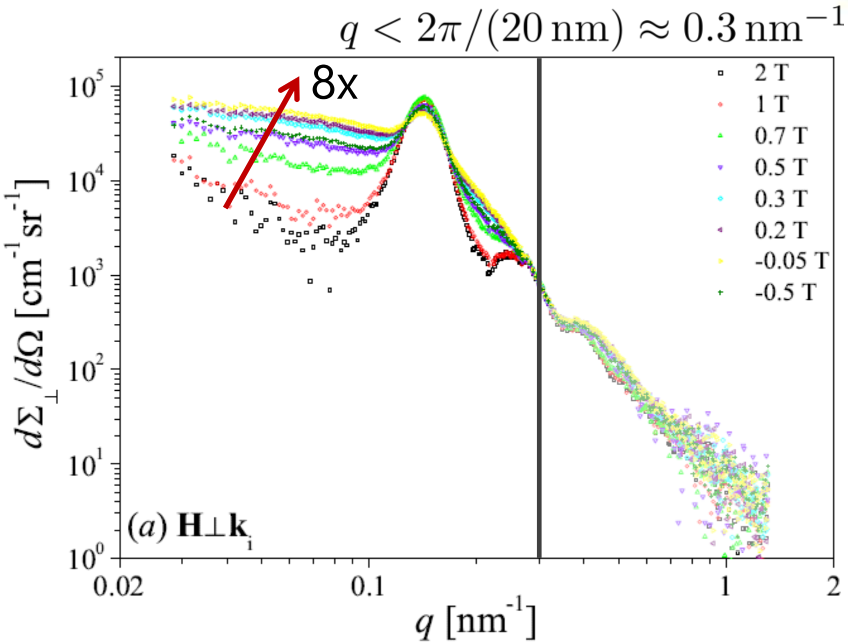

- Strong field dependent (magnetic) SANS
- Effect of
  Dipolar shape anisotropy
  Magnetocrystalline anisotropies
  polycristalline nature of rod
  Magnetostatic stray field

Summary and conclusions

- SANS probes for characteristic structural and magnetic lengths on nanometer scale
- Micromagnetic theory is a tool for the quantitative analysis of magnetic SANS
    - reproduces observed scattering anisotropy
    - H_K / ΔM determines scattering
    - approach provides quantitative information on magnetic parameters (A, H_K, ΔM)
- Dipolar interactions must be taken into account
    - Challenge remain for dense nanomagnets in nonmagnetic matrix

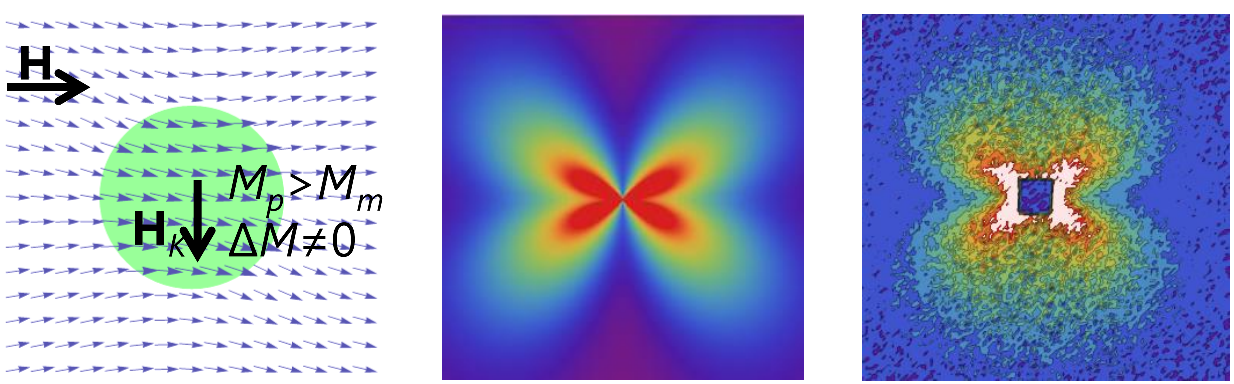

Acknowledgement

- University of Luxembourg
  Jens-Peter Bick, Frank Döbrich, Annegret Günther, Elio Perigo, Philipp Szary and Andreas Michels
- Sample preparation
  Cristina Gómez-Polo, Universidad Pública de Navarra
  Kiyonori Suzuki, Monash University
- Instrument responsibles
  Charles D. Dewhurst and Albrecht Wiedenmann, Institute Laue-Langevin
  Artem Feoktystov, Henrich Frielinghaus and André Heinemann, FRM II
  Joachim Kohlbrecher, Jorge Gavilano, Paul-Scherrer Institut
  Elliot P. Gilbert, Bragg Institute - ANSTO

uni.lu UNIVERSITÉ DU LUXEMBOURG

Fonds National de la Recherche Luxembourg

DFG

Thank you very much for your attention

D33: Modes of Operation

- Monochromatic mode with velocity selector (dλ/λ~ 10%)
- TOF mode using choppers

Spectrum of cold neutrons

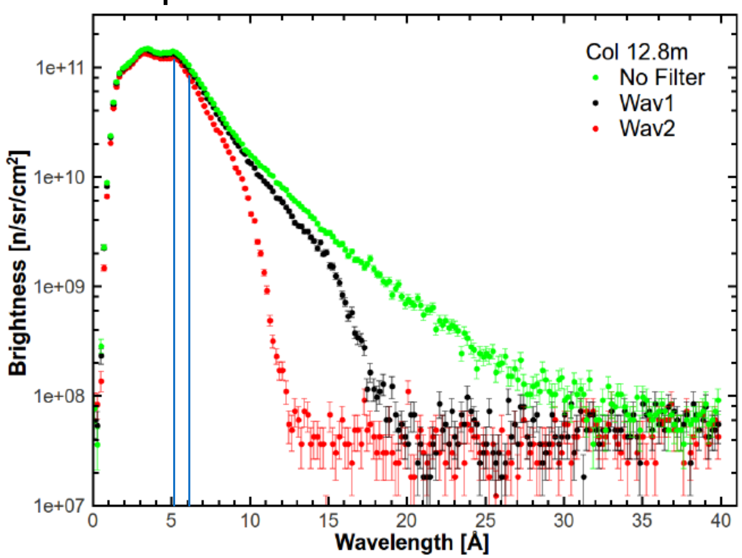

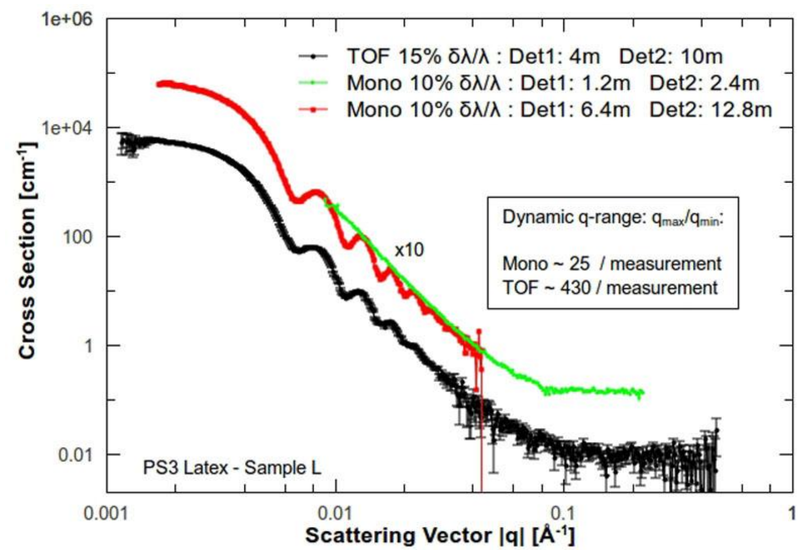

Covered q-range (probed length scales) given by sample-detector distance & wavelength
-TOF: wide simultaneous *q* range, tunable dλ/λ, but low transmission of chopper system
-Monochromatic: smaller dynamic *q* range, need for several detector distances, higher flux

Scattering length density

Neutrons

- distinguish between different elements and isotopes (e.g. H_2O vs D_2O): labelling/contrast variation
- possess a spin: sensitive to **magnetic structure**

  comparable strength of nuclear and magnetic SLD

Magnetic SLD of Co

$\rho_{mag} = b_H \, M_{s,Co} = 4.06$

$\mu_0 M_{s,Co} = 1400$ kA/m

$b_H = 2.9 \times 10^8$ A^{-1} m^{-1}

Example: Co/SiO_2 nanoparticle dispersion in water

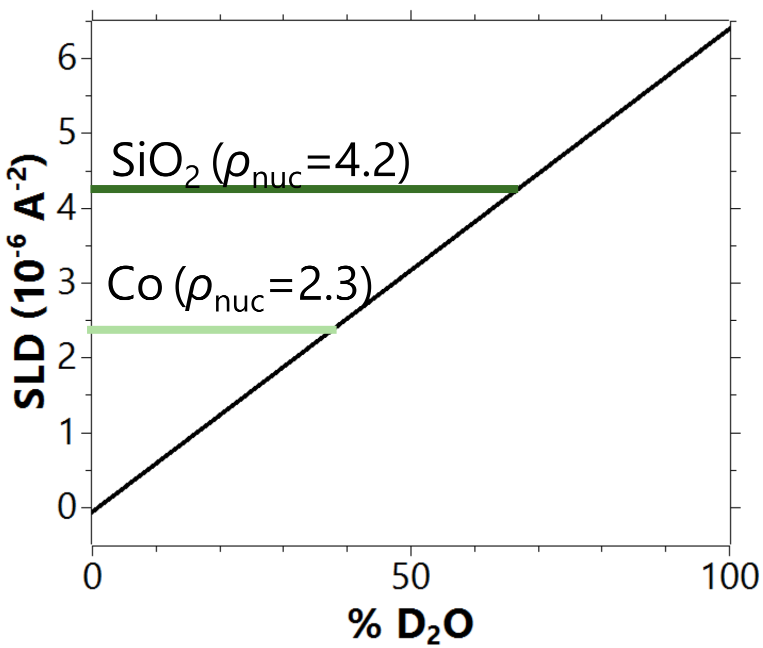

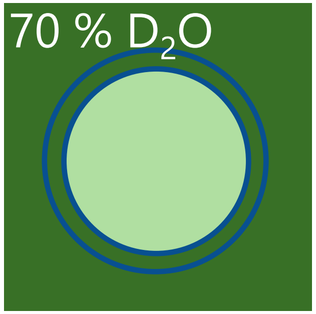

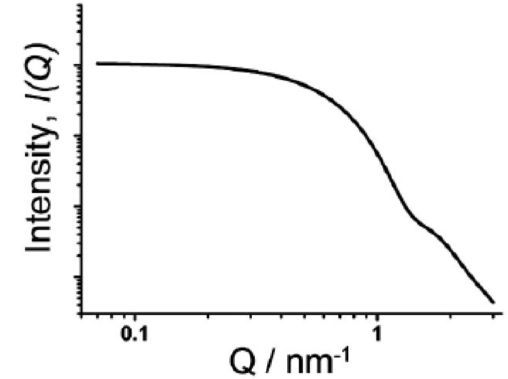

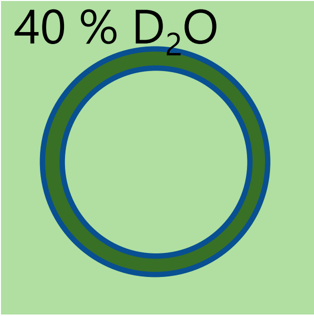

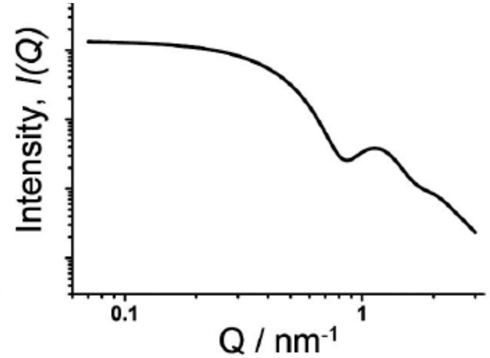

Spin-misalignment scattering

Material: $Fe_{89}Zr_7B_3Cu_1$; particle volume $\eta \approx 40$ %; particle size D = 12±2 nm

$$\frac{d\Sigma}{d\Omega}(\mathbf{q}) \propto |\widetilde{N}|^2 + |\widetilde{M}_z|^2 \sin^2\theta + |\widetilde{M}_x|^2 + |\widetilde{M}_y|^2 \cos^2\theta - 2\widetilde{M}_y\widetilde{M}_z \sin\theta\cos\theta$$

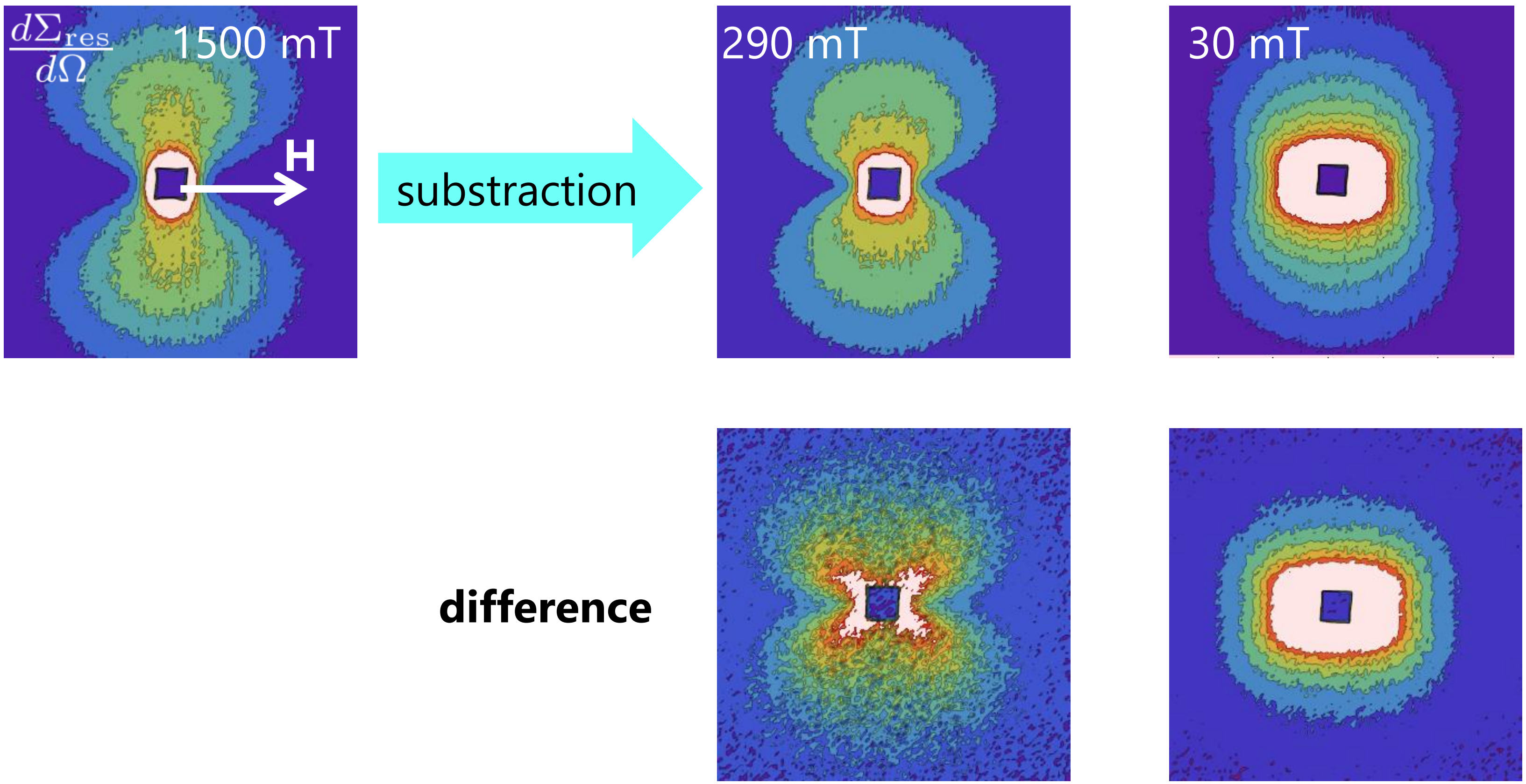

Field dependence of spin-misalignment scattering

$$\frac{d\Sigma_{\text{mag}}}{d\Omega}(q,\theta,H) \propto H_K^2\, R_K(q,\theta,H) + \Delta M^2\, R_M(q,\theta,H)$$

high H: dominated by ΔM — low H: dominated by H_K

two phases
$H_K = \Delta M$

single phase
$\Delta M = 0$

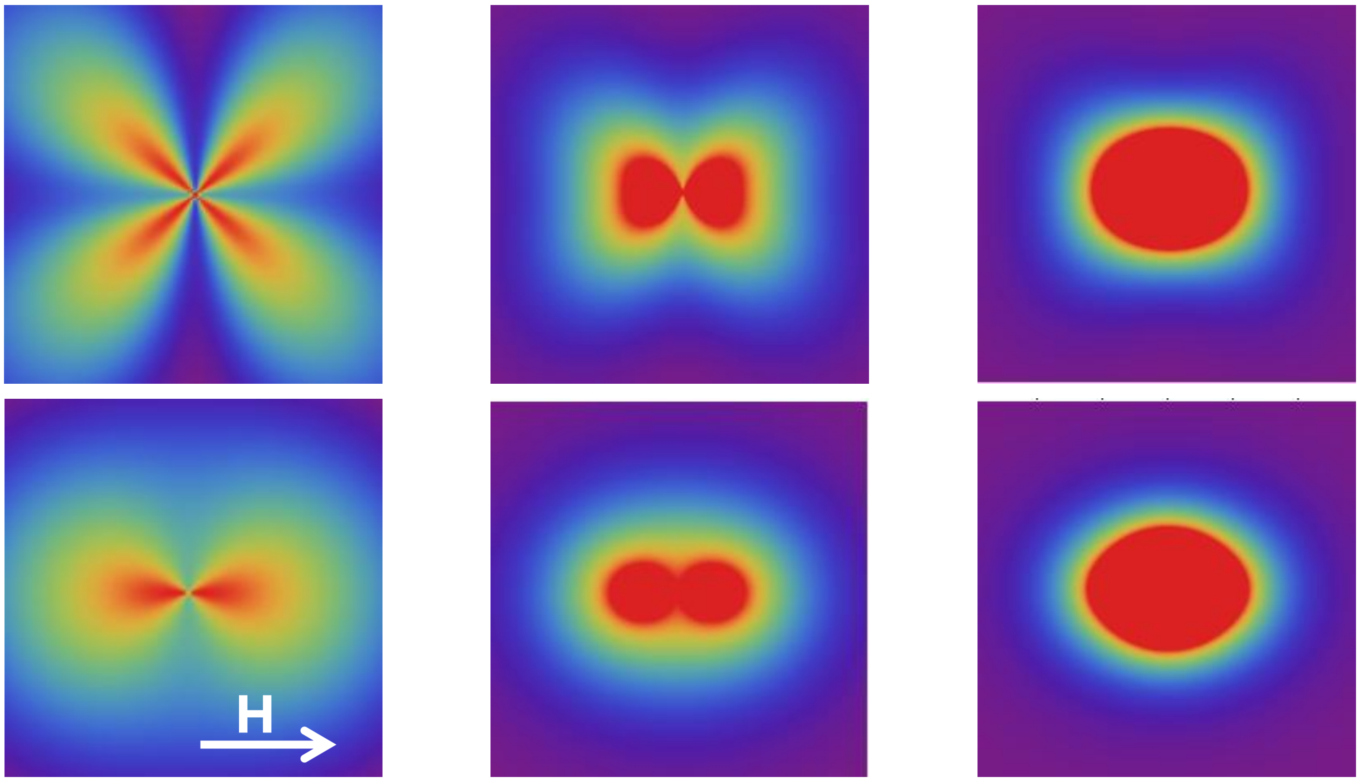

Dipolar stray fields due to ΔM in heterogeneous ferromagnets give rise to clover-leaf anisotropy

Crossover from H_K to ΔM dominated scattering

$H_K = \Delta M$

$$H_{\mathrm{eff}} = H + \frac{2A}{\mu_0 M_s} q^2$$

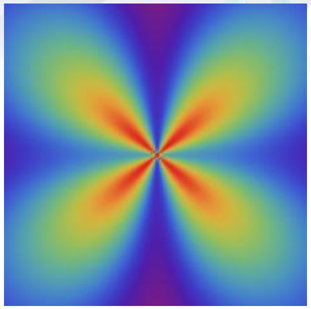

high H
$R_M > R_K$

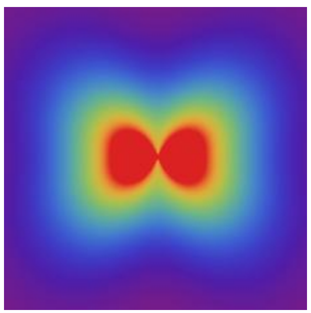

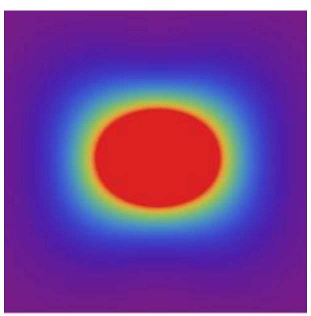

low H
$R_K > R_M$

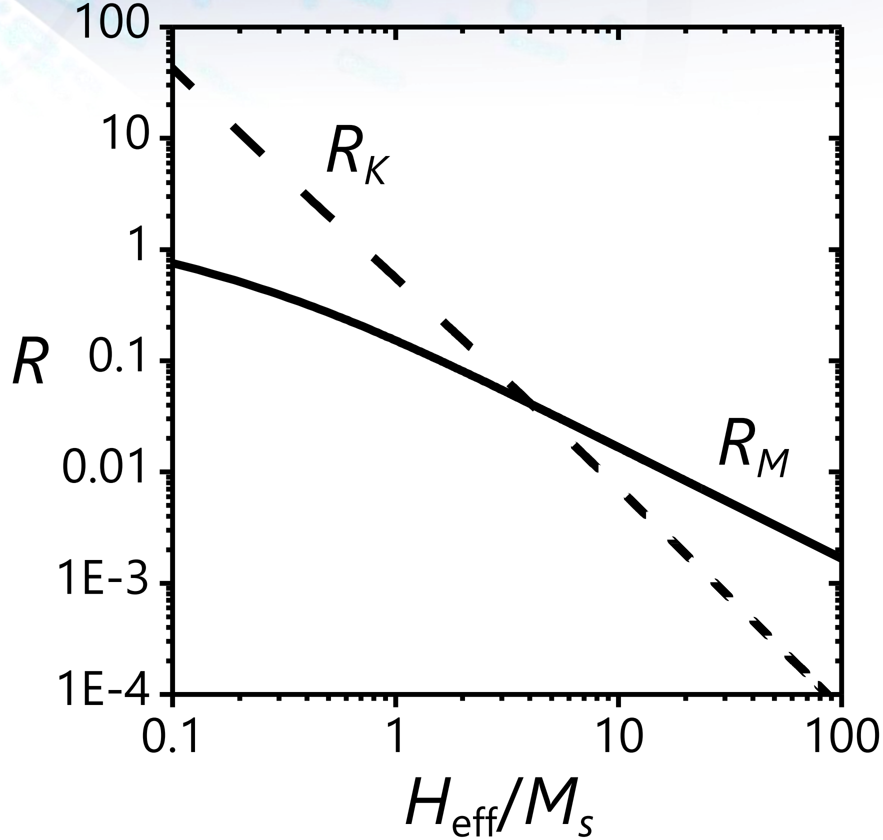

$$\frac{d\Sigma_{\mathrm{mag}}}{d\Omega}(q, \theta, H) \propto H_K^2 \, R_K(q, \theta, H) + \Delta M^2 \, R_M(q, \theta, H)$$

Micromagnetic fit procedure

spin-misalignment scattering cross section

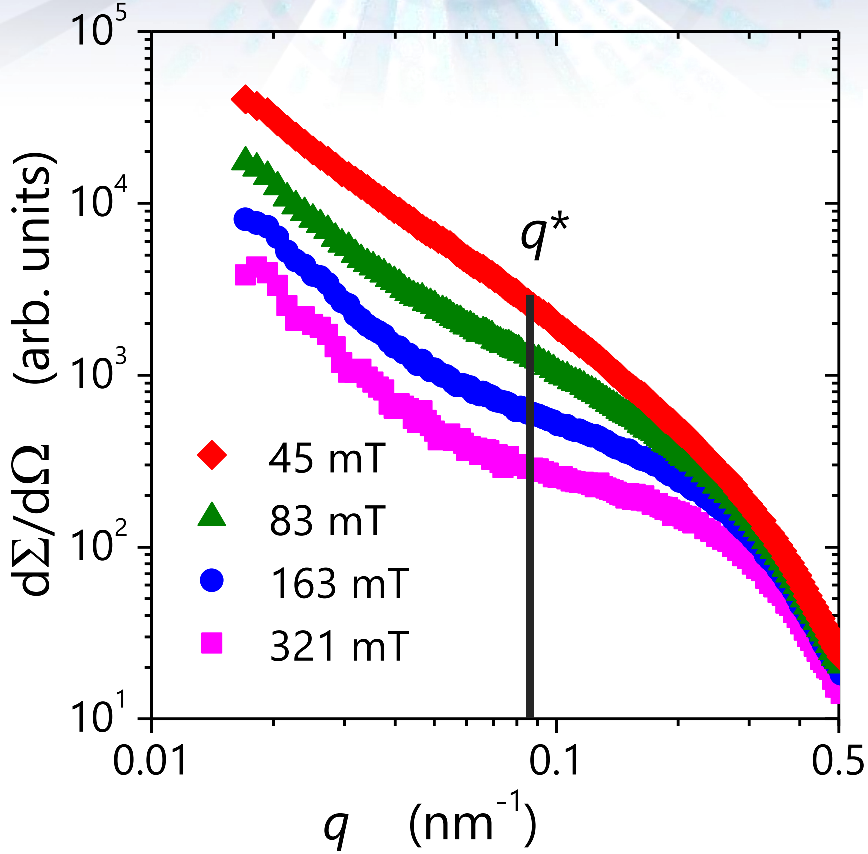

best fitting plane

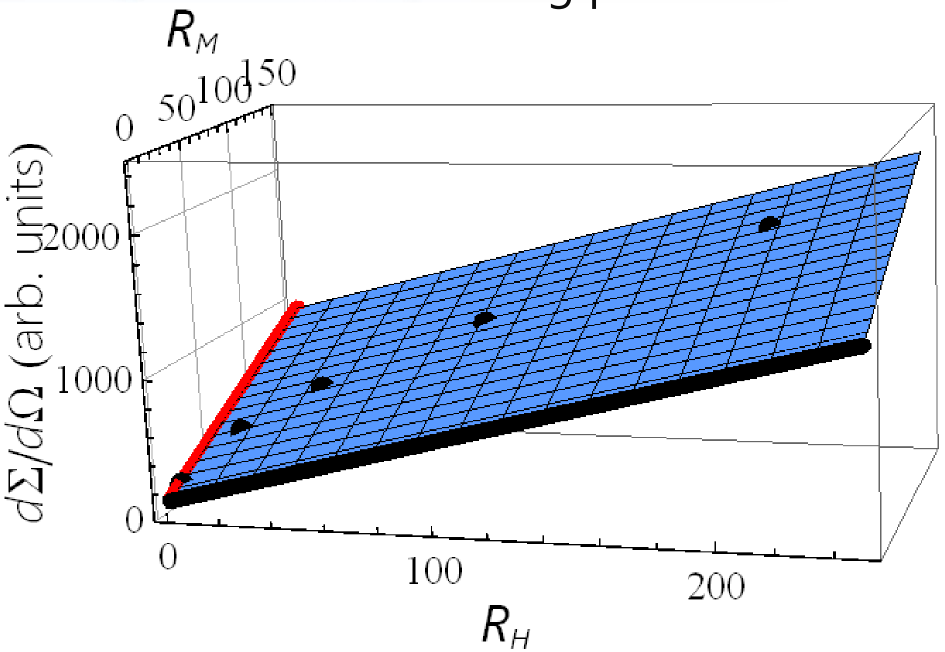

$$\frac{d\Sigma_{\mathrm{mag}}}{d\Omega}(q,H) \propto H_K^2\, R_K(q,H) + \Delta M^2\, R_M(q,H)$$

Comparison to experiment: NANOPERM

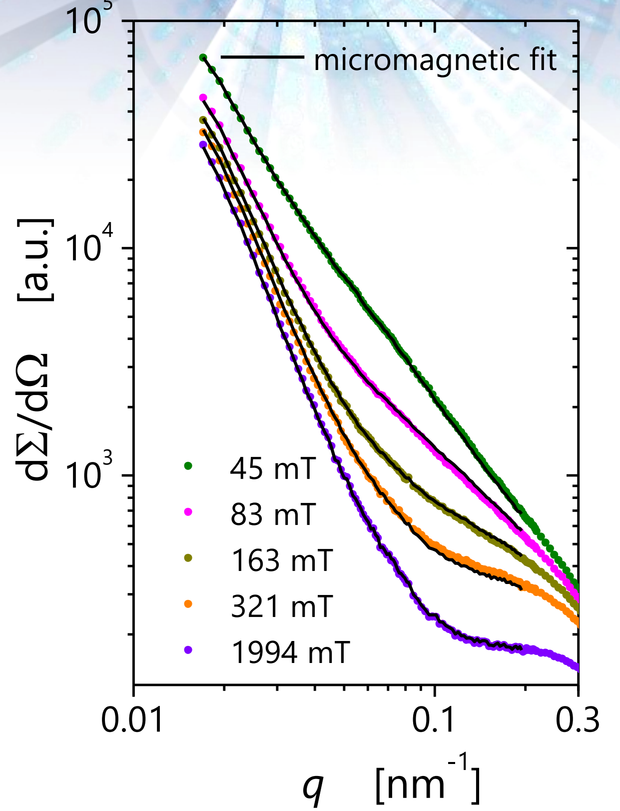

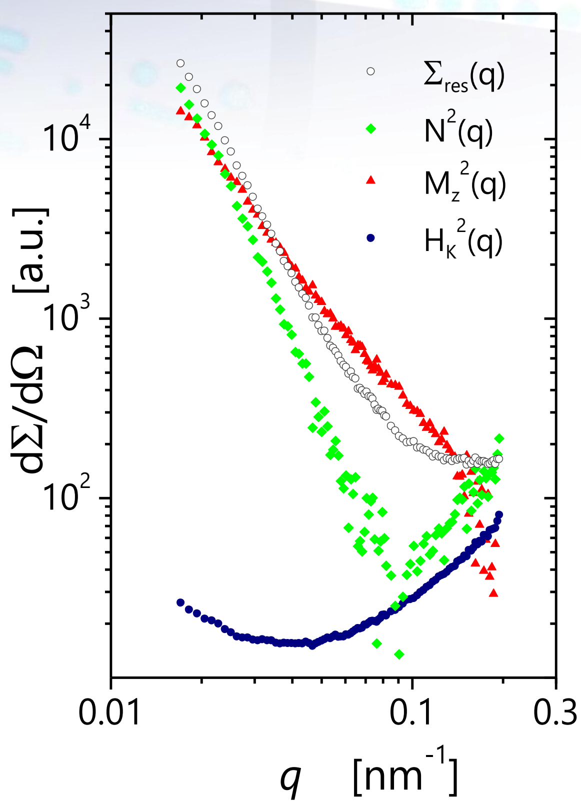

- strong spin-misalignment scattering
- exchange stiffness constant A= 4 pJ/m
- $|\widetilde{M}_z|^2$ causes major part of magnetic SANS

Single phase material

Material: electrodeposited, nanocrystalline Co; grain size D = 10±3 nm

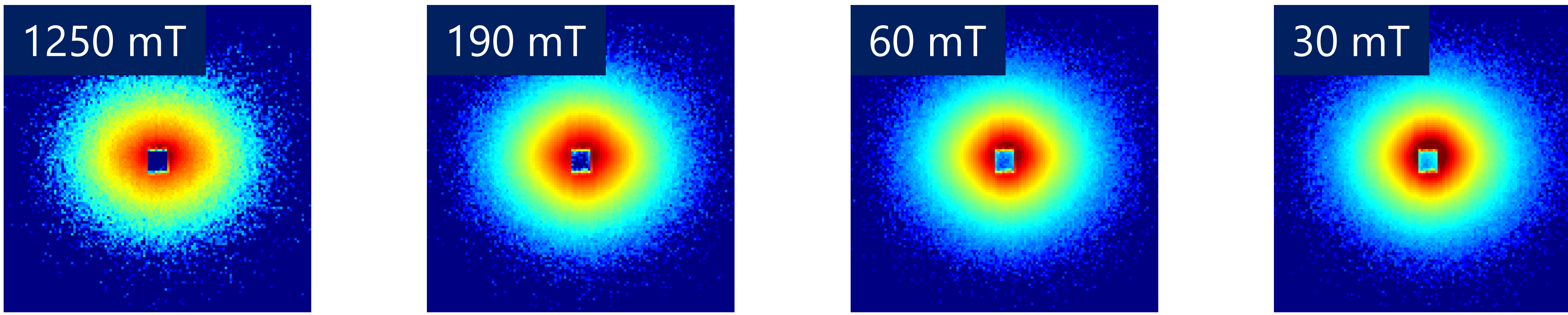

- strong spin-misalignment scattering even at highest field
- data analysis done using micromagnetic theory

Single phase material

Material: electrodeposited, nanocrystalline Co; grain size D = 10±3 nm

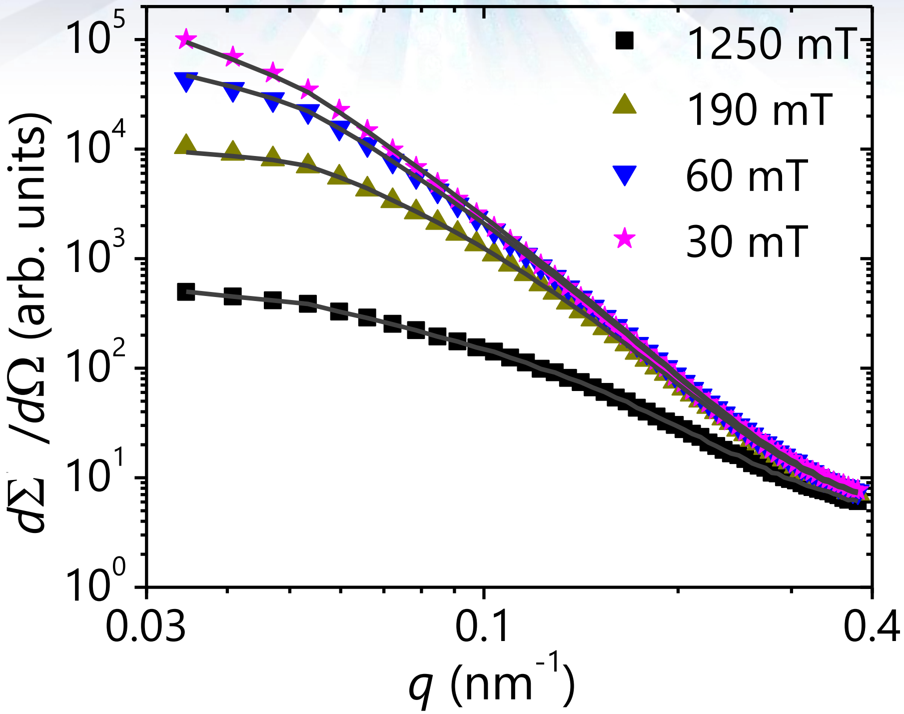

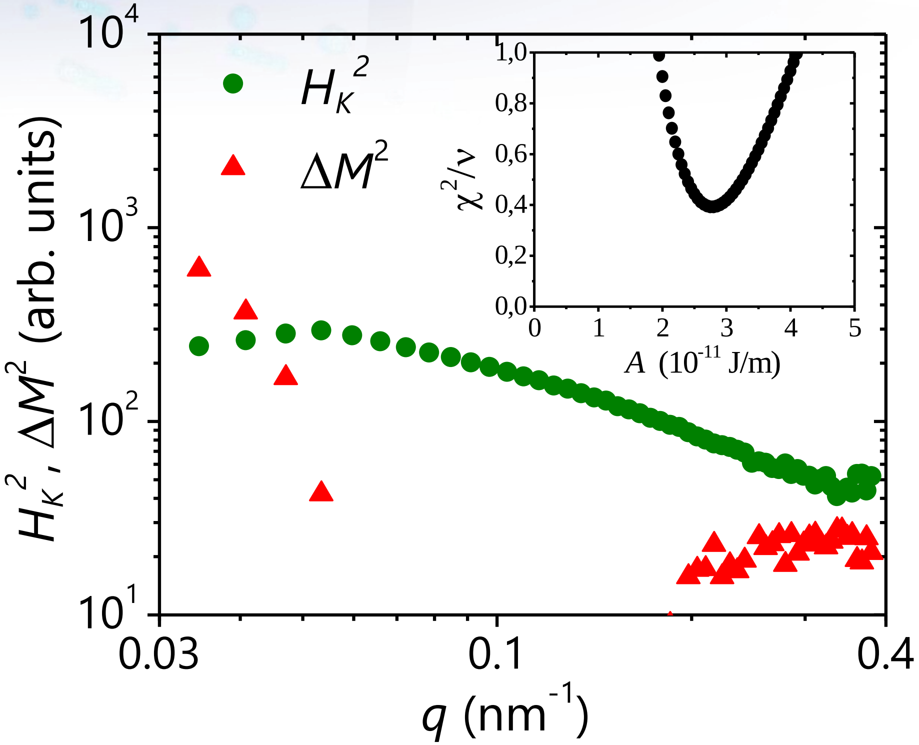

- strongly field dependent magnetic scattering
- exchange stiffness constant A= 28±1 pJ/m
- internal interfaces have no impact on exchange coupling

Nanocrystalline soft magnetic alloys

Magnetic properties
- high saturation magnetisation ($\mu_0 M_s$=1.2-1.8 T)
- high initial permeability (μ_i=10^3-10^5)
- low coercivity (H_c=1-50 A/m)

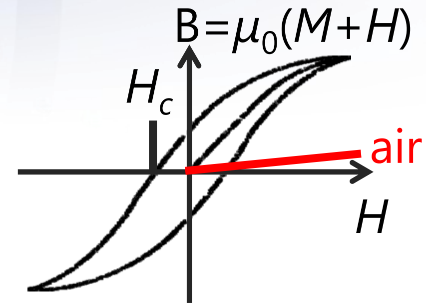

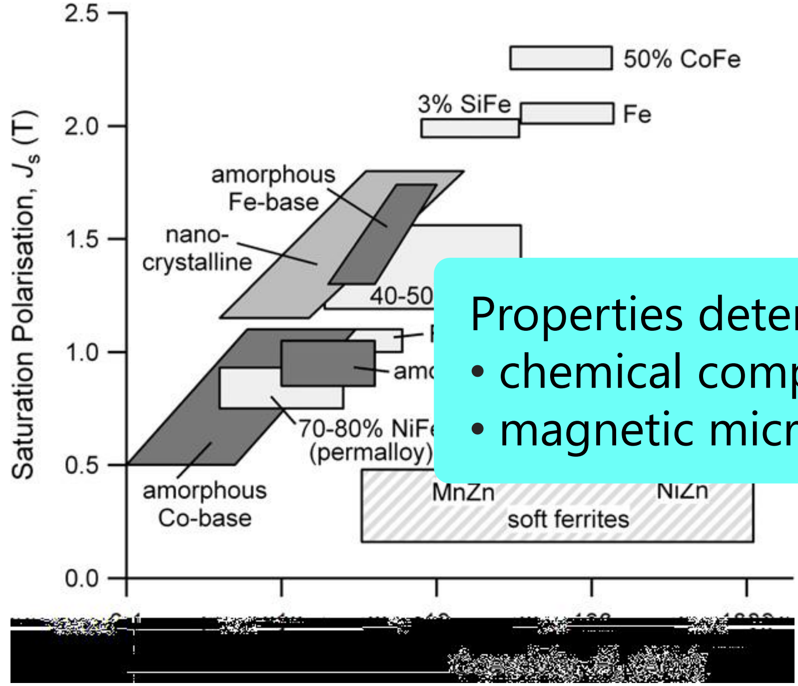

G. Herzer, Acta Materialia 61, 718 (2013)

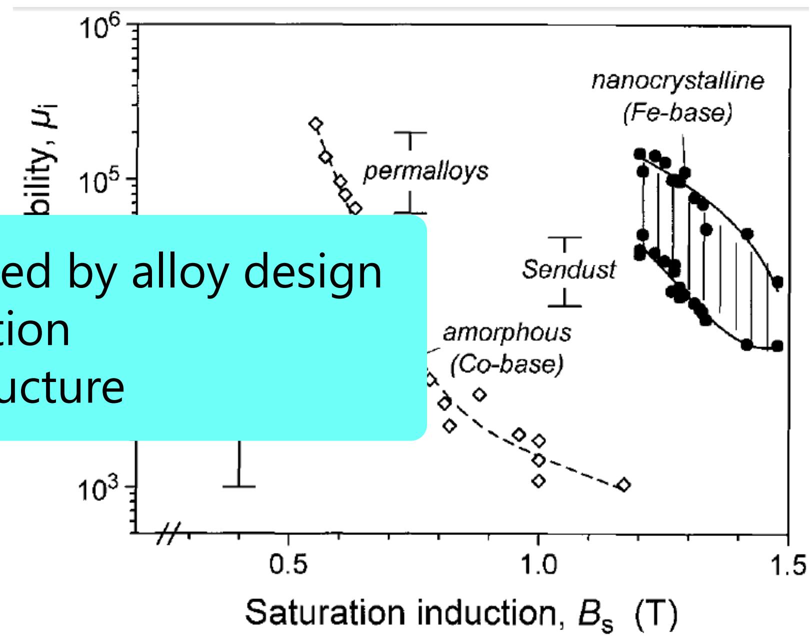

G. Herzer in Handbook of Magnetic Materials, Vol.10 (1997)

Properties determined by alloy design
- chemical composition
- magnetic microstructure

POLARIS Technique

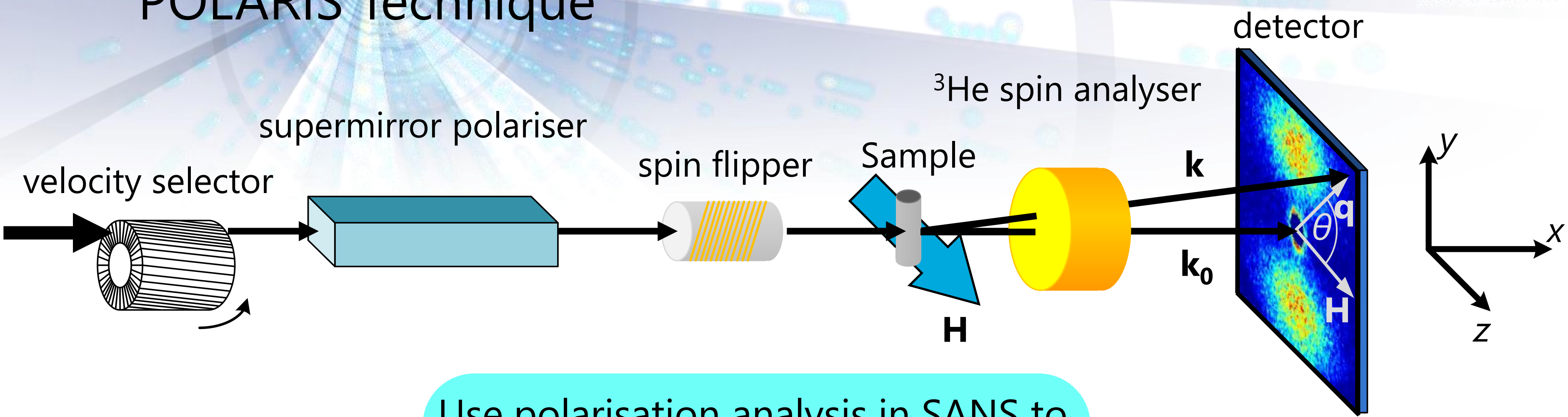

Use polarisation analysis in SANS to
- separate scattering contributions

SF channel contains
- no nuclear coherent scattering
- magnetic SANS

Spin-Flip (SF)

$$\frac{d\Sigma^{\pm\mp}}{d\Omega}(\mathbf{q}) \sim |\widetilde{M}_x|^2 + |\widetilde{M}_y|^2 \cos^4\theta + |\widetilde{M}_z|^2 \sin^2\theta\cos^2\theta - (\widetilde{M}_y\widetilde{M}_z^* + \widetilde{M}_z\widetilde{M}_y^*)\sin\theta\cos^3\theta$$

Halpern & Johnson (1939), Maleyev (1959), Blume (1963), Moon, Riste, Koehler (1969), ...

Example: Cross section of Fe-Cr-based nanocomposite

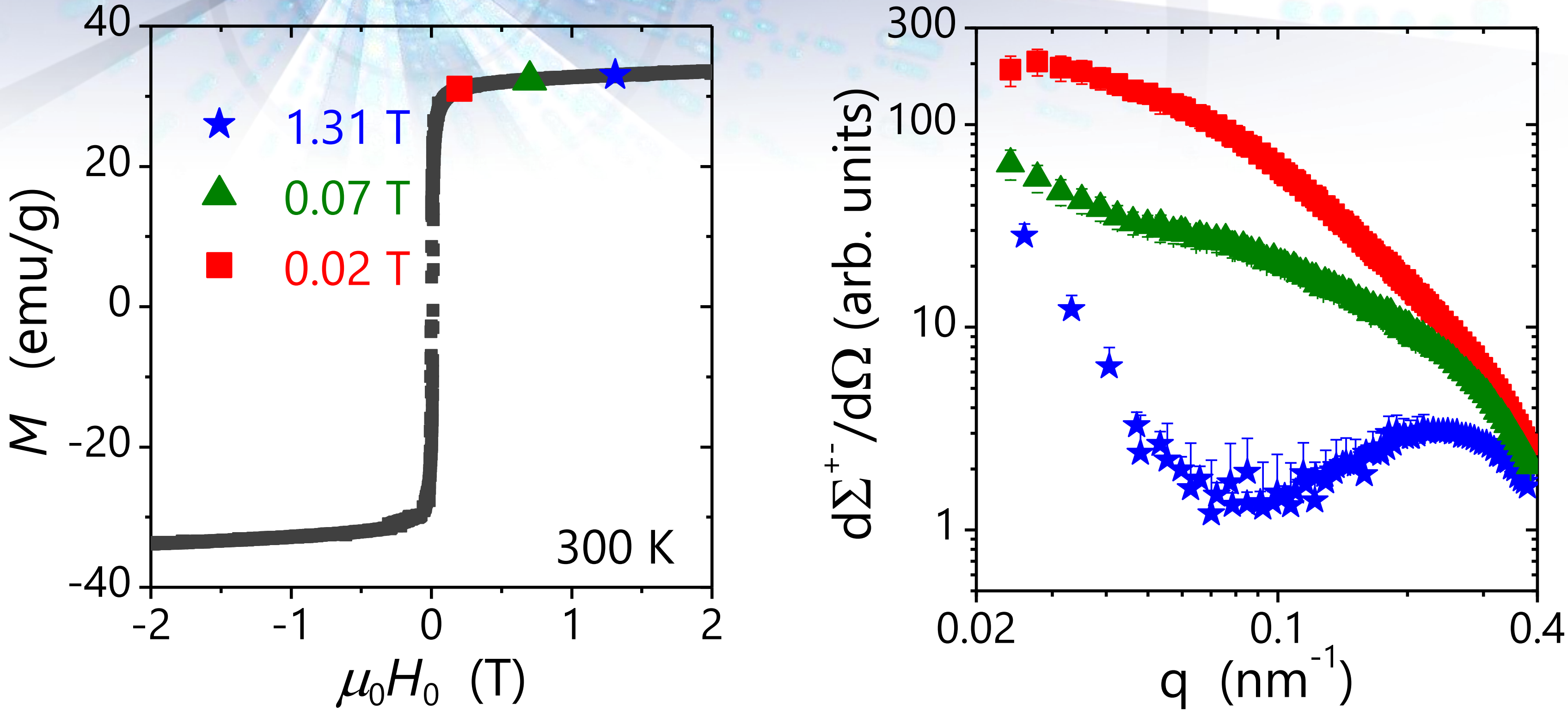

$$\frac{d\Sigma^{+-}}{d\Omega}(\mathbf{q}) \propto |\widetilde{M}_z|^2 \sin^2\theta\cos^2\theta + |\widetilde{M}_x|^2 + |\widetilde{M}_y|^2\cos^4\theta - 2\widetilde{M}_y\widetilde{M}_z\sin\theta\cos^3\theta$$

In the regime of magnetic saturation

- strongly field-dependent spin-misalignment scattering (dilute, non-interacting particle approach not appropriate)

Example: SF cross section of Fe-Cr-based nanocomposite

Material: $Fe_{63.5}Cr_{10}Si_{13.5}B_9Cu_1Nb_3$; particle size D = 14 ±2 nm; particle volume $\eta \approx 30$ %

D. Honecker et al., Eur. Phys. J. B 76, 209 (2010)

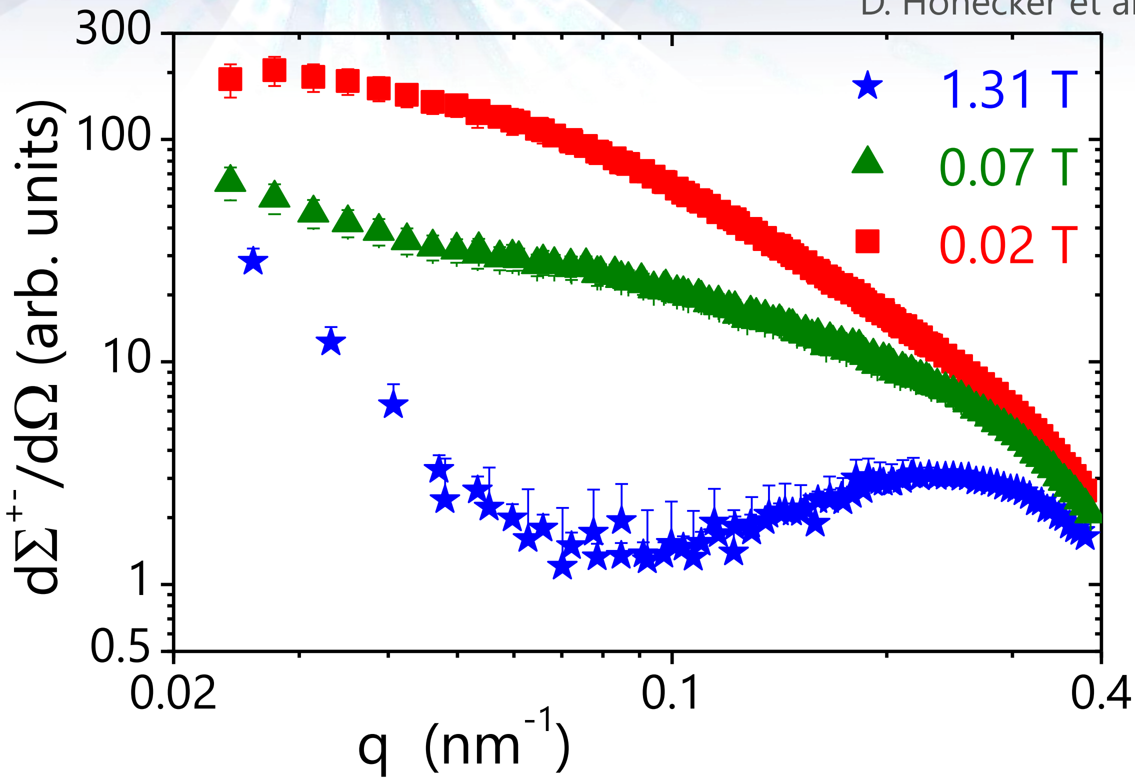

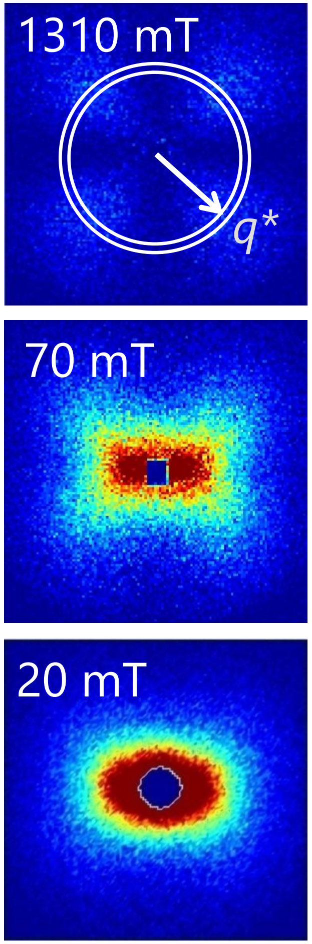

• strongly field dependent scattering

$$\frac{d\Sigma^{+-}}{d\Omega}(\mathbf{q}) \propto |\widetilde{M}_z|^2 \sin^2\theta\cos^2\theta + |\widetilde{M}_x|^2 + |\widetilde{M}_y|^2\cos^4\theta - 2\widetilde{M}_y\widetilde{M}_z\sin\theta\cos^3\theta$$

Results on a two-phase Fe-Cr-based melt-spun nanocomposite

- $Fe_{63.5}Cr_{10}Si_{13.5}B_9Cu_1Nb_3$
- FeSi-particle size D = 10-15 nm
- particle volume $\eta \approx 30$ %

C. Gómez-Polo et al., J. Magn. Magn. Mater. 316, e876 (2007)

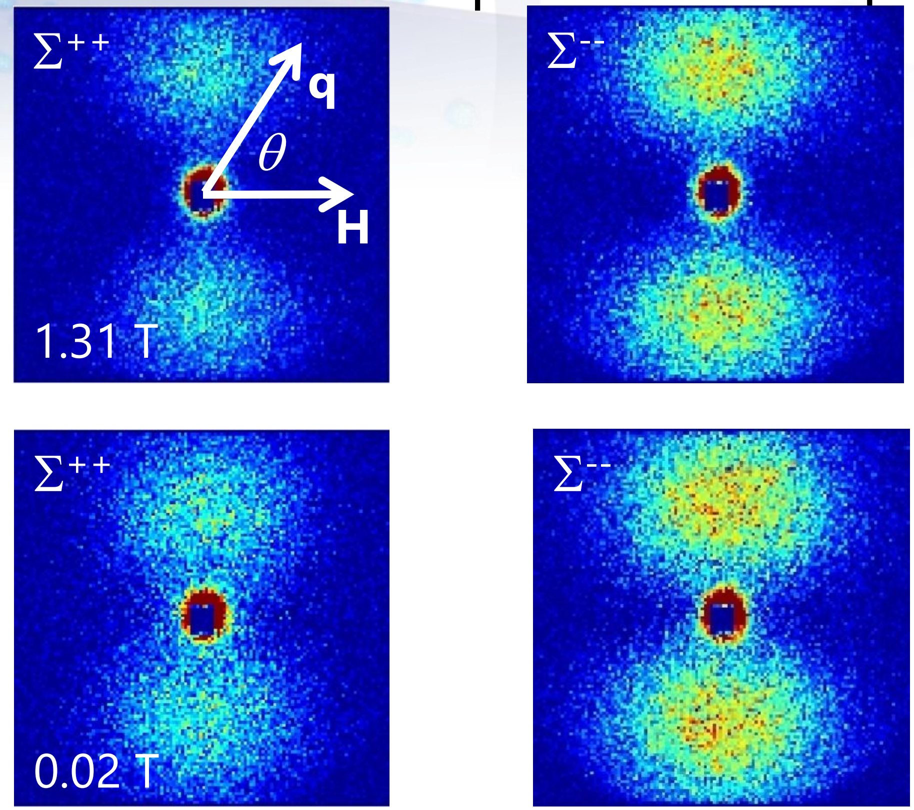

reducing field strength
- presence of transversal magnetisation components
- spin-misalignment scattering

$$\frac{d\Sigma^{\pm\pm}}{d\Omega}(\mathbf{q}) \propto |\widetilde{N}|^2 + |\widetilde{M}_z|^2 \sin^4\theta \mp (\widetilde{N}\widetilde{M}_z^* + \widetilde{N}^*\widetilde{M}_z)\sin^2\theta$$

$$+ |\widetilde{M}_y|^2 \sin^2\theta\cos^2\theta - (\widetilde{M}_y\widetilde{M}_z^* + \widetilde{M}_z\widetilde{M}_y^*)\sin^3\theta\cos\theta$$

$$\pm (\widetilde{N}\widetilde{M}_y^* + \widetilde{N}^*\widetilde{M}_y)\sin\theta\cos\theta$$

Correlation function of the spin-misalignment: theory

Sphere (R=5 nm)

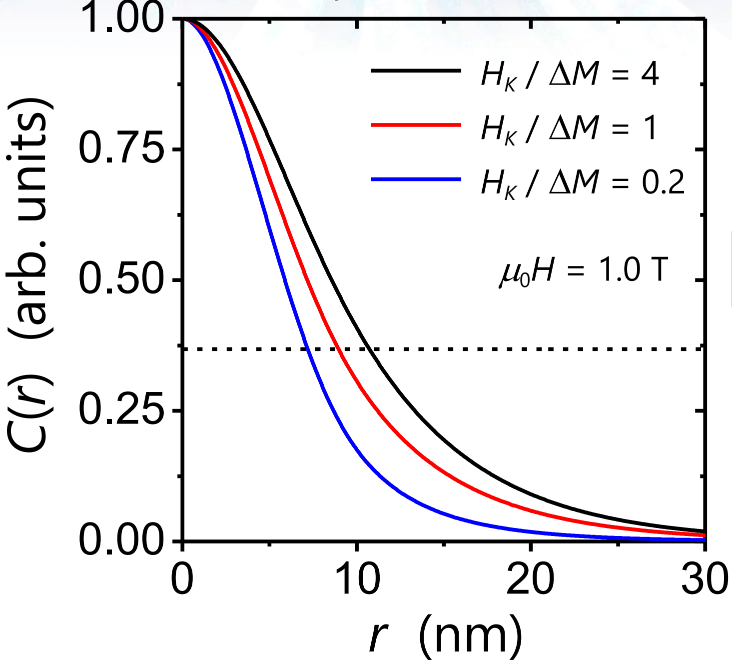

$C(l_C) = C_0/e$

Correlation decay length l_C

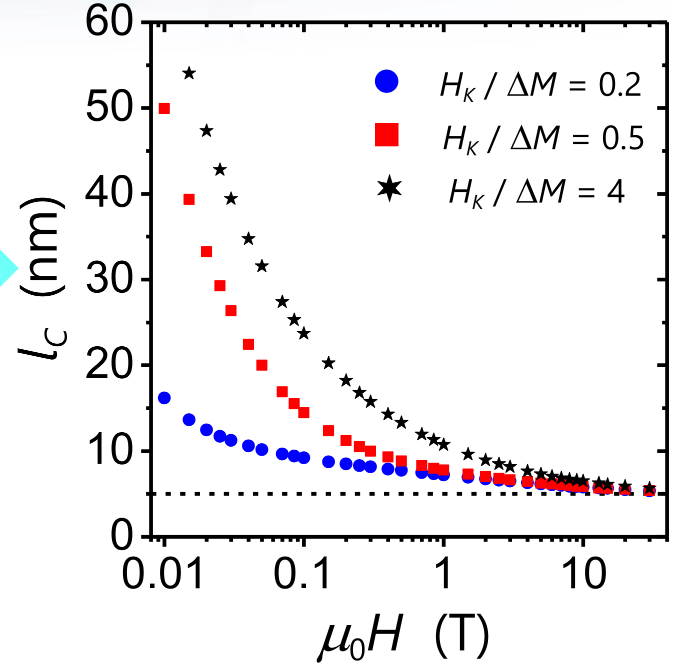

$$C(r,H) \propto \frac{1}{r}\int_0^\infty \frac{d\Sigma_{\mathrm{mag}}}{d\Omega}(q,H)\,\sin(qr)\,q\,dq$$

- ratio H_K / ΔM determines $l_C(H)$
- $l_C(H)$ approaches R for H > 1